Heliyon 10 (2024) e31832

Contents lists available at ScienceDirect

Heliyon

journal homepage: www.cell.com/heliyon

Research article

Optimal location of PMUs for full observability of power system using coronavirus herd immunity optimizer

Mohammed A. Alghassab[a,**], Ahmed Y. Hatata[a,b,*], Ahmed H. Sokrana[c], Magdi M. El-Saadawi[b]

[a] *Department of Electrical Engineering, College of Engineering, Shaqra University, Al-Dawadmi, Riyadh, 11911, Saudi Arabia*
[b] *Dept. of Electrical Engineering, Faculty of Engineering, Mansoura University, Egypt*
[c] *Egyptian Electricity Transmission Company "EETC", Delta Zone, Protection Sector, Egypt*

A R T I C L E I N F O

Keywords:
PMU
Coronavirus herd immunity optimizer
Wide-area monitoring
Fault location
Fault observability
Zero injection buses

A B S T R A C T

Phasor measurement units (PMU) are currently considered as an essential step toward the future smart grid due to their capability in increasing the power system's situation awareness. Due to their high costs and limited resources, optimal placement of PMUs (OPP) is an important challenge to compute the minimum number of PMUs and their optimal distribution in the power systems for achieving full monitoring. The coronavirus herd immunity optimizer (CHIO) is a novel optimization algorithm that emulates the flock immunity strategies for the elimination of the coronavirus pandemic. In this research, the CHIO is adapted for the OPP problem for full fault observability. The proposed algorithm is implemented on power systems considering the zero injection bus impacts. A program is created in MATLAB® environment to implement the proposed algorithm. The algorithm is applied to different test systems including; IEEE 9-bus, 14-bus, 30-bus, 118-bus, 300-bus, New England 39-bus and Polish 2383-bus. The proposed CHIO-based OPP is compared to some exact and metaheuristic-based OPP techniques. Compared to these techniques, the promising results have proved the effectiveness and robustness of the proposed CHIO to solve the OPP problem for full fault observability.

Abbreviations

Abbreviations	Nomenclature		
BIP	Binary Integer Programming	n	Problem size for CHIO
CHIO	Coronavirus Herd Immunity Optimizer	*CL*	Number of cross-links related to bus *j* in N-bus system
CO	Cuckoo Optimization	$V_{p,R}$	Voltage at any point *p* measured from the receiving end
C-19BOA	COVID-19-based optimization algorithm	$V_{p,S}$	Voltage at any point *p* measured from the sending end
CVO	Coronavirus optimization	D	Per-unit fault location index
DE	Differential Evolution	Z_c	Characteristic impedance
GA	Genetic Algorithm	γ	Propagation constant
GPS	Global Positioning System	*L*	Transmission line length
HISS	Herd Immunity Search Space	*x*	Variable vector defined for the optimization problem

(*continued on next page*)

* Corresponding author. Department of Electrical Engineering, College of Engineering, Shaqra University, Al-Dawadmi, Riyadh, 11911, Saudi Arabia.
** Corresponding author.
E-mail addresses: malghassab@su.edu.sa (M.A. Alghassab), ahmed_hatata@su.edu.sa (A.Y. Hatata).

https://doi.org/10.1016/j.heliyon.2024.e31832
Received 27 January 2024; Received in revised form 3 May 2024; Accepted 22 May 2024
Available online 23 May 2024

(*continued*)

ILP	Integer Linear Programming	M	Number of radial buses in the N-bus system
MAE	Mean Absolute Error	BR_r	Original spreading rate for CHIO
MILP	Mixed Integer Linear Programming	Max_{AGE}	Death rate of infected cases
OPP	Optimal Pmu Placement	C_0	Initial infection rate, default set to 1
PSO	Particle Swarm Optimization	PoS	Size of studied people
PMU	Phasor Measurement Unit	h_p	Decision variable indexed by p within available e decision variables for a case
RMSE	Root Mean Square Error	l_b, u_b	Minimum and maximum limits of h_p
SQP	Sequential Quadratic Programming	Max_Itr	Iterations number for CHIO
TL	Transmission Line	y, z	Sequence admittance and impedance per unit of distance for the TL
ZIB	Zero Injection Bus		

1. Introduction

In the era of global positioning system (GPS) satellites, digital signal processing, and communication technologies, it is entirely possible to observe the electric power systems' operation [1]. The synchronized signals of the GPS satellite system used by the Phasor Measurement Units (PMUs) have evolved into sophisticated tools that are manufactured commercially [2]. Due to their improved accuracy and high sampling rate for measuring phase angles, PMUs have been widely accepted in electric power systems for wide-area control, protection, and monitoring [3,4]. The advanced applications of PMUs in power systems can improve their reliability and security [5].

A power system is considered observable if all voltage phase angles and magnitudes at all buses can be uniquely estimated, given a finite set of measurements. If the PMUs are located at all buses in the grid, and all measurements are transmitted to the control center, then the voltage and current phasors are known for all buses and transmission lines (TLs) [6]. However, the power system can be fully monitored in the case that PMUs are located on a definite number of buses whenever the phasor voltages at the buses without PMUs are determined by utilizing the power grid parameters and the PMUs' measurements of the other buses. These buses are called quasi-measurement buses [7].

It is well known that the overhead TLs and underground cables are subjected to faults continuously. So, minimizing their outage periods is essential to ensure power system reliability and continuity. Thus, fast, and accurate fault detection, identification, and location should be considered as vital targets for power system operators [8–12]. Nowadays, several algorithms of fault location based on the PMU techniques for transmission systems have been conducted [13,14]. These algorithms determine fault location using the synchronized phasors' current and voltage. They can attain very high accuracy in locating TLs' faults if the PMUs are located on every bus [13]. However, for economic and technical considerations, it is impracticable to place the PMUs on all buses of the power system. These considerations include some factors such as; measuring channels' numbers, grounding connections of the power station, voltage/current transformers, and antenna connections, but the major factor restraining the number of PMUs installed is their price and the communication equipment cost that may be higher than the PMU itself [14]. Communication limitations and the high price of the PMUs have encouraged electrical developers and mathematicians to search for the optimal number and locations of PMUs for different desired purposes.

Optimal PMU Placement (OPP) has been studied by applying different algorithms to attain full observability of power systems during normal and abnormal operating conditions [15–27]. A literature review of different optimization techniques applied to solve the OPP problem was presented in Ref. [15]. A simple method-based Integer Linear Programming (ILP) was applied for optimal placement of PMUs in a power system [16]. To achieve complete power system observability, ILP was used in Ref. [17] to determine the OPP. The method was based on the bus-to-bus connection matrix that made the observability of the power system simpler. A multi-stage placement procedure of PMUs using the Mixed Integer Linear Programming (MILP) was presented [18]. Two stages; dual-stage algorithm and fuzzy decision-making were used to arrange the multiple solutions. The OPP was determined on Oman power system using the GAMS under the CPLEX solver and the MILP model [19]. An OPP approach for power system observability considering several contingencies was introduced [20]. The effect of both single branch outages and PMU outages on the OPP problem was studied. In Ref. [21], a hybrid-optimization technique combined with local search and branch-and-bound procedure based on the interior-point method was introduced for solving the OPP problem.

In power systems, a Zero-Injection-Bus (ZIB) is any bus that has no load or generation connected to it. ZIB's measurements can be obtained non-directly from any other bus connected to it, which may be helpful to provide an additional reduction of the required number of PMUs. In Ref. [22], Binary Integer Programming (BIP) was applied to resolve the OPP considering the zero injection buses (ZIBs) to achieve topological observability of the power system. An effective solution for the OPP problem by considering the zero injection measurements was obtained by applying MILP [23]. An integrated model considering the effects of the ZIBs and conventional measurements on PMU placement was presented to obtain a feasible solution [24]. In Ref. [25], a hybrid algorithm of minimum spanning tree and genetic algorithm (GA) was applied to compute the minimum installed number of the PMUs for completely observing the power system. The minimum spanning tree algorithm was used for modifying the unobservable solution into observable solutions, while the GA was applied to fix any unobservable buses of the allocated PMUs. Both Particle Swarm Optimization (PSO) and Cuckoo Optimization (CO) were applied to identify the optimal number and placements of the PMUs while achieving associated restrictions [26]. Whereas, PSO and Global search optimization techniques were applied to solve the OPP problem [27].

Many researchers have discussed the OPP scheme for locating faults in power systems [28–34]. Ref. [28] presented a proposed fault location algorithm that depended on the measurements of the synchronized phasor voltages at both faulted TL terminals and the phasor currents fed from one terminal. Although the measurements detected an accurate fault location for the studied system, the manual technique used to detect PMUs' locations may be difficult for larger power systems. Besides, the possibility of ZIBs in the power system was not considered in that study. An OPP algorithm to observe and detect faults was proposed in Ref. [29], but it was not comprehensive, and consequently, moreover, it gave inaccurate results.

It is predicted that the observable power systems during normal operation may be unobservable under faulty conditions due to the changes in the system configuration as an extra bus (fault-point) is created in the faulty system. Researchers in Refs. [30–34] have discussed this problem to obtain the optimal placement and minimum number of PMUs for full system observability in both normal and faulty conditions. In Ref. [30], the located PMUs were used to detect the fault by one terminal current and voltage data. Whereas, in Ref. [31] GA was used to calculate the minimum number and optimal locations of the PMUs for wide-area fault locations determined from terminal voltage measurement. Moreover, the algorithm was applied to optimize the number of PMUs in order to identify the fault points along with the longitude and latitude [32]. A hierarchical clustering technique was applied in Ref. [33] to split the power system into coherent areas to determine the most relevant buses to attain complete power system observability during faults. Then the optimal PMUs' locations were determined for every area depending on simple rules. A fault-tolerance-based approach to OPP was presented in Ref. [34]. The proposed approach considered the vulnerability and observability of the system and PMUs.

In late 2019, the world was hit by a severe pandemic (Covid-19) which claimed many lives. Study and analysis of the behavior of COVID-19 have inspired a lot of optimization algorithms such as coronavirus optimization algorithm [35], COVID-19-based optimization algorithm (C-19BOA) [36], Coronavirus optimization (CVO) [37], and coronavirus herd immunity optimizer (CHIO) [38]. While these algorithms proved an encouraging execution in treating optimization issues, CHIO may be considered as the most efficient because of its flexible and adaptable control parameters which allow effective investigating and exploring of search areas [39]. So, in this paper, the CHIO is used to solve the OPP problem considering zero injection buses. The technique is implemented on various IEEE standard systems and the results are compared to previously utilized optimization techniques.

The main contributions of this research can be summarized as:

1. Define the optimal PMU placement including the objective function and its constraints for achieving a full fault observable network.
2. Apply a novel effective meta-heuristic algorithm, CHIO, to solve the OPP problem for full fault observable transmission networks, while studying the enhancement of the optimal solution by considering ZIB impact.
3. Compare the proposed CHIO-OPP algorithm with other methods (ILP, PSO, Differential Evolution (DE), and Sequential quadratic programming (SQP)) based on the PMUs' optimal number and their locations.
4. Evaluate statistically the performance of the applied fault location technique compared with another published technique.

The rest of the paper is structured as follows: Section 2 gives a brief discussion on fault observability analysis based on PMU. Section 3 formulates the PMU placement problem. Section 4 illustrates the procedures for applying the CHIO. Section 5 presents a proposed method for determining the optimal number of PMUs and their locations based on fault observability. Case studies and results are presented and discussed in Section 6. Finally, Section 7 concludes the paper.

2. Fault observability analysis based on PMU

One of the main features of transmission systems is that they are fault-observable systems. They can detect and locate any occurred fault directly based on the available measured data. However, not all observable systems within healthy operating conditions remain observable in fault conditions due to the changes in the configuration of the TL under faulty conditions as a new bus is added at the fault point.

2.1. Rules of fully fault-observable transmission networks

In this study, the following rules are considered in fault observability analysis using PMUs These rules are derived from Refs. [33, 40,41].

Rule 1 For any TL to become fault-observable, information on both end buses' voltage phasors and the phasor of fault current fed from its two terminals should be available.
Rule 2 Whenever a PMU is located at any bus, the phasor voltage of that bus and the phasor currents of all TLs connected to that bus are measurable.
Rule 3 The availability of both current and voltage phasors at any terminal of a TL makes it possible to determine the voltage phasor at the other terminal of this line.
Rule 4 If the voltage phasors of the two terminals of any TL are available, the current phasor in this TL can be determined.
Rule 5 ZIB is a bus that has no load or generation connected to it. Thus, at any ZIB there are no injected currents into the system, which means that the summation of currents flowing through all TLs connected to this bus is zero.
Rule 6 The voltage phasor of any ZIB can be obtained if both the current and voltage phasors of the other terminal of any TL related to this ZIB are available.

2.2. Description of the applied fault location algorithm

The one-line diagram of a two-terminal single-circuit TL is illustrated in Fig. 1. The receiving and sending ends are denoted by subscripts R and S respectively [42–45].

A symmetrical components transformation matrix is used to split the quantities of a 3-phase TL considering distance variation (kilometers) only. The relations between both currents and voltages at the fault location, F, (at distance f from bus R) can be calculated by Eqs. (1) and (2).

$$\frac{\partial V_{012}}{\partial x} = z_{012} * I_{012} \tag{1}$$

$$\frac{\partial I_{012}}{\partial x} = y_{012} * V_{012} \tag{2}$$

where y_{012} and z_{012} are the sequence admittance and impedance per unit distance correspondingly. It is noticed that both z_{012} and y_{012} matrices are diagonal matrices with diagonal entries (z_0, z_1, z_2) and (y_0, y_1, y_2), respectively. Besides, V_{012} and I_{012} represent the voltage and current matrices where $V_{012} = [V_0 \quad V_1 \quad V_2]^T$ and $I_{012} = [I_0 \quad I_1 \quad I_2]^T$. The subscripts 0, 1, and 2 depict the zero, positive, and negative sequences, correspondingly.

The voltage and current at any point p at a distance 'a' from bus 'R' can be expressed by Eqs. (3) and (4).

$$V_{p1} = A_1 * e^{(\gamma * a)} + B_1 * e^{-(\gamma * a)} \tag{3}$$

$$I_{p1} = \frac{1}{Z_c}\left[A_1 * e^{(\gamma * a)} + B_1 * e^{-(\gamma * a)}\right] \tag{4}$$

where $Z_c = \sqrt{z/y}$ and $\gamma = \sqrt{z * y}$ are the characteristic impedance and the propagation constant, respectively. The currents and voltages at the sending and receiving ends are used as boundary conditions to calculate the constants of the 2nd-order differential equations (3) and (4), i.e. A_1 and B_1.

The voltage at point p with respect to the sending and receiving ends in (3) can be reformulated as:

$$V_{p1,R} = \frac{V_{1,R} + Z_c * I_{1,R}}{2} e^{(\gamma * a)} + \frac{V_{1,R} - Z_c * I_{1,R}}{2} e^{-(\gamma * a)} \tag{5}$$

$$V_{p1,S} = e^{-\gamma * L} \frac{V_{1,S} + Z_c * I_{1,S}}{2} e^{(\gamma * a)} + e^{\gamma * L} \frac{V_{1,S} - Z_c * I_{1,S}}{2} e^{-(\gamma * a)} \tag{6}$$

The positive-sequence quantities are selected to compute the fault locations in this paper as these quantities can react to all types of faults. Equations (5) and (6) denote the positive sequence voltage at fault point (F), which are determined with respect to the measured ($V_{1,S}$, $I_{1,S}$) and ($V_{1,R}$, $I_{1,R}$) at both sending and receiving ends, respectively.

Assume that a fault happens at a distance $f = D*L$ (km) from bus R, where "D" and "L" represent the per-unit fault location index and TL length. By equalizing the voltages measured from both sending and receiving ends at point "F"; i.e. $V_{F,R} = V_{F,S}$ and equating (5) and (6), the index "D" can be determined by Eqs. from (7) to (9).

$$D = \frac{\ln\left(\frac{Q}{M}\right)}{2 * \gamma * L} \tag{7}$$

where

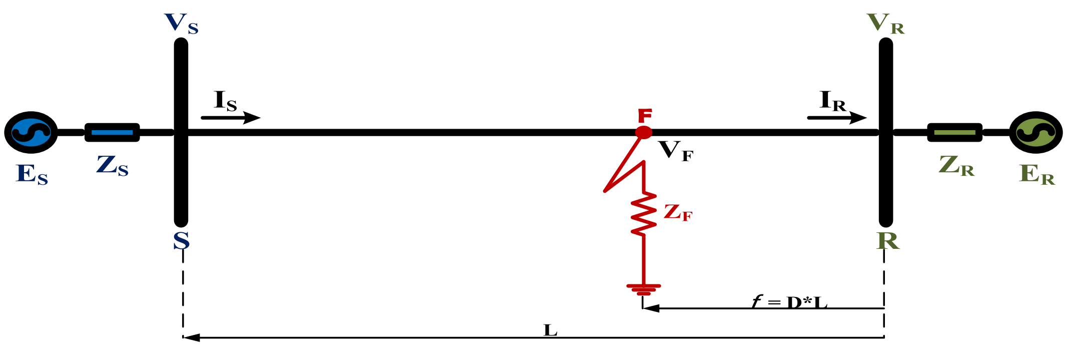

Fig. 1. One-line diagram of a single-circuit TL.

$$M = \frac{1}{2} * \left((V_S + Z_c * I_S) * e^{-\gamma * L} - (V_R + Z_c * I_R) \right) \tag{8}$$

$$Q = \frac{1}{2} * \left((V_R - Z_c * I_R) - \ (V_S - Z_c * I_S) * e^{\gamma * L} \right) \tag{9}$$

In this case, whenever the fault point is located between bus R and S of the TL, then D will be within the range [0, 1]. Otherwise; the D value will be undefined. As shown in Eqs. from (7) to (9) neither loading conditions, such as source impedance, and loading change, nor fault conditions, i.e., occurrence angle, impedance, and type, have any effect on fault location index, D.

3. Formulation of the OPP problem

The OPP problem aims to determine the optimal number of the PMUs and their locations which guarantees the full observability of a system under any fault condition.

3.1. Objective function

The optimization problem objective is to obtain the optimal locations of the PMUs by minimizing their number in the system. Equation (10) modeled the objective function, *f(x)* [40];

$$f(x) = min \left(\sum_{i=1}^{N} x_i \right) \quad i = 0, 1, \ldots, N \tag{10}$$

where N represents the bus number of the power system, and x is a variable vector defined for the optimization problem whose entries as x_i. The value of x_i (taken as one or zero) indicates whether the PMU is located at bus i or not.

3.2. Problem constraints

After formulating the objective function, it is essential to define its linear and nonlinear constraints. Firstly, the types of buses and TLs in any power system that are used for OPP problem are: a) Terminal bus is any bus which connected to the rest of the bus system through an individual TL, b) Radial buses are the buses connected radially to ZIBs through radial links, and c) Cross-links are the TLs that connecting radial buses to each other's. Then, considering or ignoring the presence of ZIBs will affect the OPP restrictions, as illustrated in the following subsections.

3.2.1. OPP constraints without considering ZIB

In this case, the rules from 1 to 4 (in section 2.1) are applied, hence the following constraints are considered:

Constraint 1: For any TL to be fault observable, a PMU must be located at any of its two terminals. So, it is essential to apply the same spaced strategy when installing PMUs in the system. Hence for the N-bus system with H transmission lines, the constraint for jth TL is represented by (11) as:

$$for\ line\ h_j : x_m | x_k \geq 1 \quad j = 1, 2, \ldots H \tag{11}$$

where m and k are the two end buses of the jth TL.

The inequality (11) denotes that a PMU is installed at either bus m, bus k, or both end buses of line j. This guarantees that at least one PMU is installed at any one of the two end busses of each TL. Accordingly, whenever a fault occurs at any TL, both current and voltage phasors at one terminal are measured whereas the voltage phasor at the other terminal is obtainable, either measured directly or calculated. This condition guarantees the full fault observability of the transmission system.

Constraint 2: For terminal buses, PMU must be placed directly. Thus, this can be expressed by (12).

$$x_i = 1 \tag{12}$$

3.2.2. OPP constraints considering ZIB

The presence of ZIBs in the transmission system is used as pseudo-information. In this case, the system will be observable during faults with a lower number of PMUs compared to the case when the ZIBs are not included. The required number of PMUs is determined depending on how the zero-injection buses are connected to the transmission system. In case the ZIBs are considered, all the above-mentioned rules from 1 to 6 (in section 2.1) are applied. In addition to the previous two constraints, the next constraints are added.

Constraint 3: When a ZIB is connected to the network through radial TLs only, the number of PMUs necessitated to observe faults in the ZIB area is the same as the number of radial TLs. The reason is that the remote buses connected to the ZIB, i.e., radial buses, are considered as terminal buses and a PMU must be installed at each of them. This is the most restraining case. Therefore, for "*M*" radial buses connected to a "*j*" ZIB, the following constraint is represented by (13):

$$x_j + \sum_{i=1}^{M} x_i \geq M \tag{13}$$

Constraint 4: When cross-links interconnect radial buses, a smaller number of PMUs is required. In this case, the radial buses are not considered as terminal buses in the ZIB zone. Hence, in general, the PMUs' numbers needed for fully observing faults in TLs linked with ZIBs will be identical to the radial buses' numbers minus cross-links. So, in case of the presence of cross-links, the last equation must be modified to (14).

$$x_j + \sum_{i=1}^{M} x_i \geq M - CL \tag{14}$$

where CL is the number of cross-links related to bus j.

By employing any optimization technique for solving the former objective function (10) subjected to the constraints specified by (11) to (14), the optimal PMUs' placements are accomplished for achieving fault observability.

4. Coronavirus herd immunity optimizer

A rapidly spread respiratory virus, COVID-19, has attacked humanity all over the world since December 2019. Lots of experiments have been done to find powerful treatments to eradicate the severe epidemic. Until this happens, flock immunity strategies are still the effective way to prevent this fatal virus from being spread. Flock immunity is achieved when many people have received their natural protection against COVID-19 infection, and this is done either if they have got vaccines or are naturally infected and treated, as illustrated in Fig. 2 [46,47]. The following steps summarize flock immunity:

1. Some susceptible people get their infection from other already infected people.
2. Immunity would be gained against coronavirus for the recovered people who represent the largest proportion, while the minority of the infected people are being died.
3. Each human has immunity and would be able to prevent this virus from being spread, and hence all people would get their self-anti-coronavirus protection.

CHIO is a recent meta-heuristic optimization algorithm in which both the COVID-19 spreading phenomenon and flock immunity strategies are considered as its main inspiration origin [36]. It consists of two main groups of parameters including controller and algorithm parameters. Controller parameters administer the CHIO's behavior and algorithm parameters establish the search area parameters. The CHIO algorithm consists of six procedural stages summarized in the flowchart shown in Fig. 3.

The six stages can be further explained as follows:

1. *Initialize CHIO parameters*: In this stage, both of controller and algorithm parameters of CHIO are initialized. The optimization problem is also initialized and can be expressed by Eq. (15).

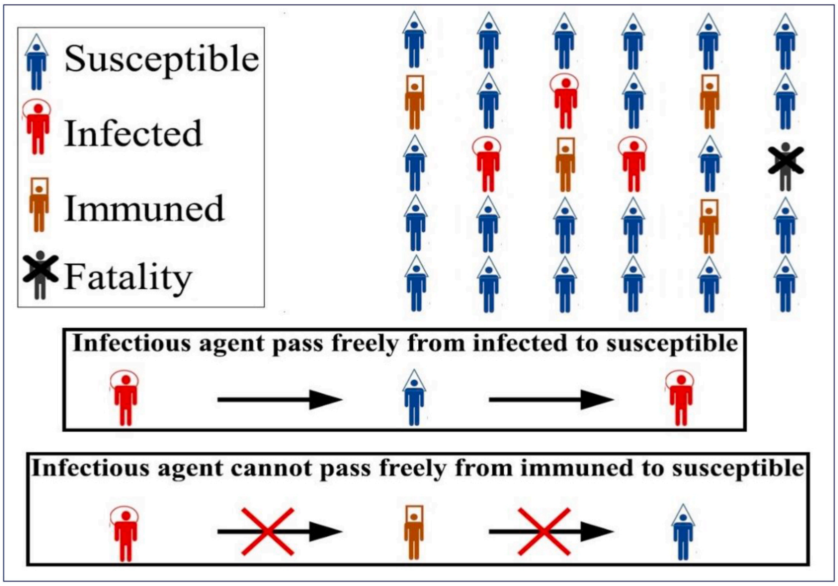

Fig. 2. Flock immunity strategy.

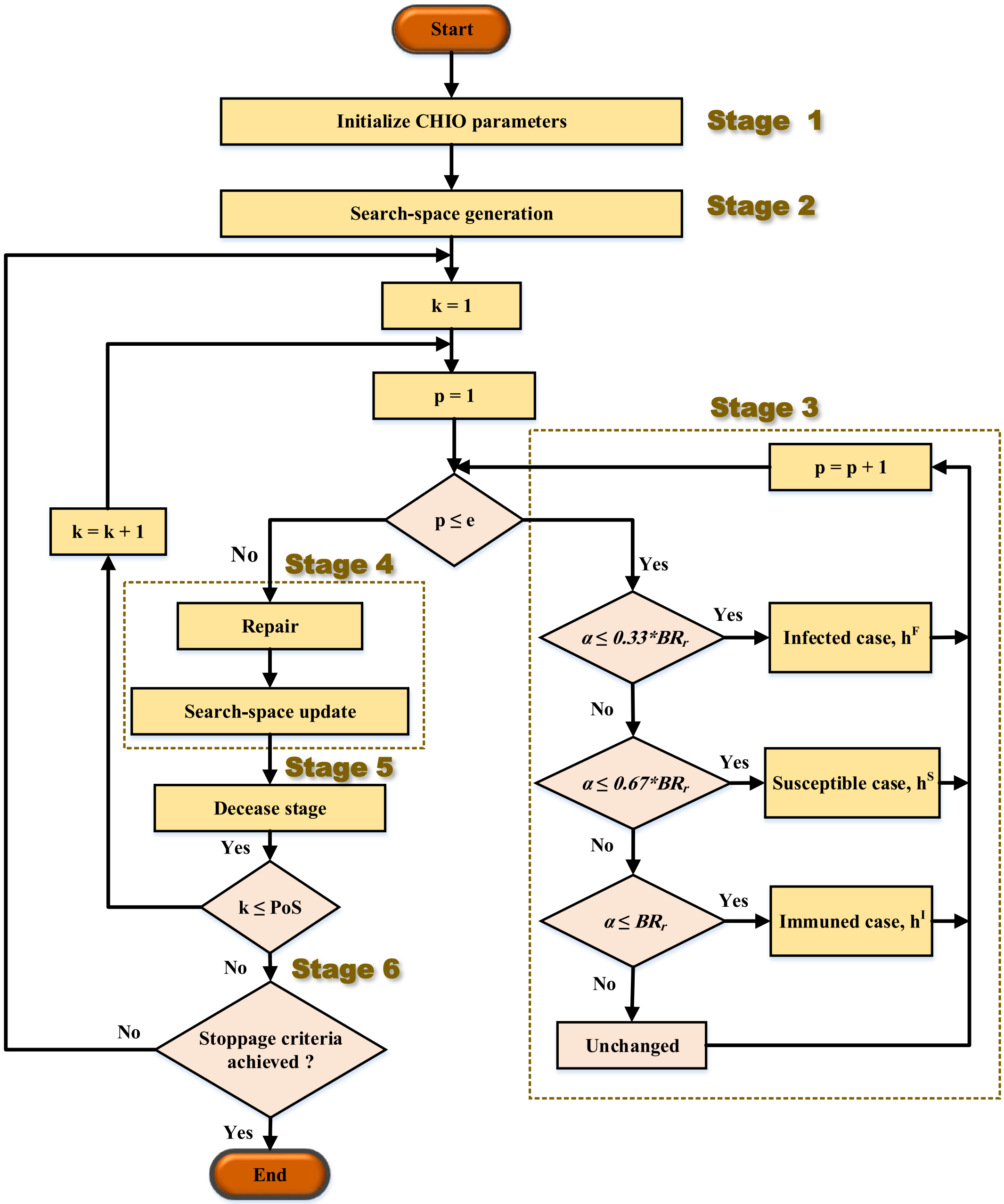

Fig. 3. CHIO algorithm flowchart.

$$\min_h f(h), h \in (l_b, u_b) \tag{15}$$

where $f(h)$ is the objective function to be solved for each person within the population (or a case) $h = (h_1, h_2, \ldots.., h_e)$ and h_p is the decision variable indexed by p within available e decision variables for every case, while l_b and u_b are the minimum and maximum limits of h_p.

2. *Search-space generation*: In this stage, a random formulation of the herd immunity search space (*HISS*) of the optimization problem is set. *HISS* can be expressed by an array as illustrated in (16).

$$HISS = \begin{bmatrix} h_1^1 & h_2^1 & \cdots & h_e^1 \\ h_1^2 & h_2^2 & \cdots & h_e^2 \\ \vdots & \vdots & \vdots & \vdots \\ h_1^{PoS} & h_2^{PoS} & \cdots & h_e^{PoS} \end{bmatrix} \tag{16}$$

where every line k represents an individual case h^k which is defined by (17).

$$h_p^k = l_{b_p} + \left(u_{b_p} - l_{b_p}\right) * U(0,1), \forall p = (1,2,\ldots,e) \tag{17}$$

where $U(0,1)$ represents a uniform random number between 0 and 1.

Equation (15) is applied for all individuals h separately to determine their objective functions (Immune rate), while, for each individual case within the *HISS*, a state vector (SV) is initiated by either 1 or 0. According to the initial infection rate size, C_0, ones are produced randomly in SV.

3. *Evolving of herd immunity*: This is the main improvement loop of CHIO. Based on the original spreading rate, BR_r, decision variables can still be constant or be affected (reduced by a factor) due to social spacing according to 3 scenarios as expressed by (18).

$$h_p^k(t+1) = \begin{cases} h_p^k(t), \alpha \geq BR_r \ (\textit{No changes}) \\ h_p^k(t) + \alpha * \left(h_p^k(t) - h_p^F(t)\right), \alpha \in \left(0, \frac{BR_r}{3}\right) \quad (\textit{Infected}) \\ h_p^k(t) + \alpha * \left(h_p^k(t) - h_p^S(t)\right), \alpha \in \left(\frac{BR_r}{3}, \frac{2 * BR_r}{3}\right) \ (\textit{Susceptible}) \\ h_p^k(t) + \alpha * \left(h_p^k(t) - h_p^I(t)\right), \alpha \in \left(\frac{2 * BR_r}{3}, BR_r\right) \quad (\textit{Immuned}) \end{cases} \tag{18}$$

where α is a random number $\in (0,1)$. For infected cases, $h_p^F(t)$ is spontaneously chosen based on the SV from each infected case h^F, hence $F = \{p|SV(p) = 1\}$. For susceptible cases, $h_p^S(t)$ is spread randomly from each susceptible individual h^S, and is centralized within SV, $S = \{p|SV(p) = 0\}$. For immunized cases, $h_p^I(t)$ represents the perfect protected individual h^I within SV such that $f\left(h^I\right) = \min_{k\sim\{K|SV(K)=2\}} f\left(h^k\right)$.

4. *Search-space update*: Determination of the objective function (Immune rate) is done for every produced case, the new solution replaces the previous one only if the immunity is enhanced, i.e., $f\left(I^k(t+1)\right) < f\left(I^k(t)\right)$. If a solution is replaced, then its Age value A^k would be incremented by 1 in case of $SV^k = 1$, i.e., infected case. Also, the SV would be updated for the produced solution according to (19) as follows:

$$SV^k = \begin{cases} 1 \quad \text{if}\, f\left(h^k(t+1)\right) < \frac{f(h)^k(t+1)}{\Delta f(h)} \,\Lambda\, SV^k = 0 \,\Lambda\, Cor\_vir\left(h^k(t+1)\right) \\ 2 \quad \text{if}\, f\left(h^k(t+1)\right) < \frac{f(h)^k(t+1)}{\Delta f(h)} \,\Lambda\, SV^k = 1 \end{cases} \tag{19}$$

where $Cor\_vir\left(h^k(t+1)\right)$ represents a binary value set to 1 via inheritance of $h^k(t+1)$ from infected individuals, and $\Delta f(h)$ denotes the individuals' fitness average rate which is expressed as $\Delta f(h) = \frac{\sum_{p=1}^{PoS} f(h_p)}{PoS}$.

5. *Decease stage*: In this stage the age of each infected case, i.e., $h^k(t+1)\,\Lambda\, SV^k = 1$), is put in a comparison with the death rate of infected cases. If ($A^k \geq Max_{AGE}$), this solution will be removed and that case will be considered dead. Then a regeneration process of a newer solution is done with setting ($A^k = 0$) and ($SV^k = 0$).
6. *Stoppage criteria*: The 3rd, 4th, and 5th stages are repeated until the pre-determined iterations number (*Max_Itr*) is reached. By reaching this condition, only immunized and susceptible individuals would appear in the search space with the elimination of those who are infected.

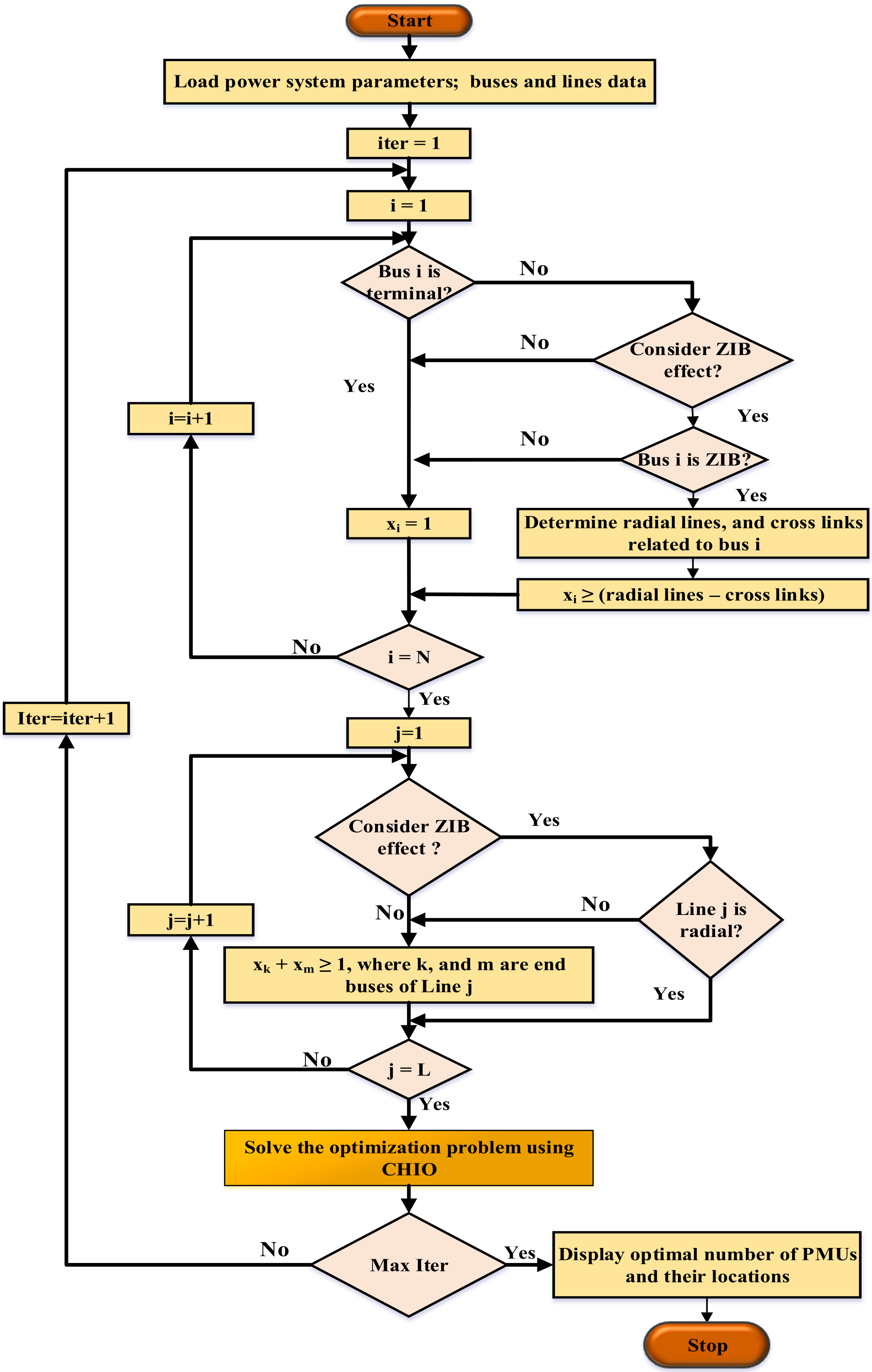

(caption on next page)

Fig. 4. Flowchart of optimal PMUs placement-based CHIO for full TL observability.

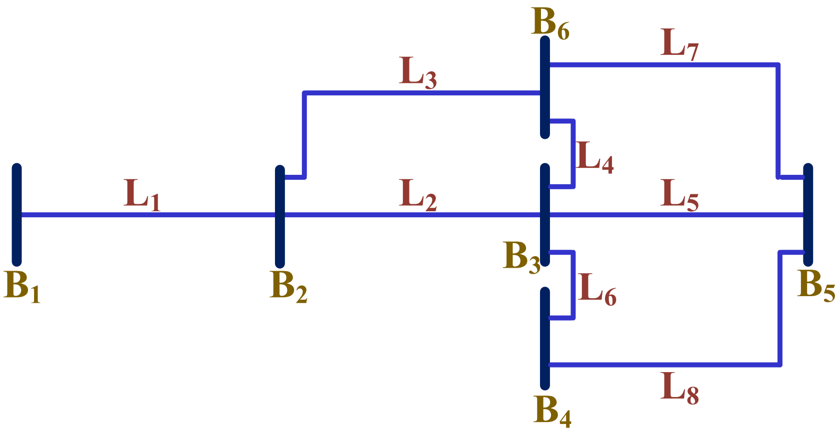

Fig. 5. Hypothetical 6-bus transmission test system.

5. Proposed CHIO for OPP

The CHIO is used to determine the minimum number of PMUs in an N-bus power system and their optimal placements for full observability. On applying the CHIO for OPP the following items are considered:

- The CHIO search agents are the buses on which the PMUs will be installed and these search agents are represented by the "N" dimension.
- The total number of the PMUs is chosen to represent the fitness function in the OPP problem.

The following steps summarize the procedure optimal PMUs placement-based CHIO for full TL observability whereas Fig. 4 depicts a flowchart to illustrate these steps.

Step 1 *Collect the system data*: Create both bus and branch matrices for the studied system. The bus matrix detects the total system buses and the locations of both generation and load buses. Whereas, the branch matrix identifies the TLs interconnecting buses and their number.

Step 2 *Prepare the required data for optimization*: Both bus and branch matrices are coded in the computational environment, which produces terminal buses, ZIBs, radial buses, and cross-links.

Step 3 *Detect terminal buses*: Each terminal bus should have a PMU installed on it, i.e., $x_i = 1$.

Step 4 *Detect ZIBs:* When considering the ZIB effect, apply the constraint of, $x_j \geq$ (radial TLs – cross-links) for any zero-injection bus, *j*, considering the cross-links related to that bus (if presented).

Step 5 *Check fault observability:* Ensure that any TL has at least one PMU located at each of its buses for fault observability, i.e., $x_m + x_k \geq 1$ where *m* and *k* are the two end buses of the TL unless this line is radial (only when considering ZIB effect).

Step 6 *Obtain the correct optimal solution:* Apply the proposed CHIO-based method to solve the OPP problem and detect the optimal number and placement of PMUs adequate for full fault observability.

Step 7 *Ensure that the obtained solution is correct*: The optimal solution is not approved unless the values of the objective function are constant for a pre-specified number of iterations, at least.

6. Results and discussion

To evaluate the proposed CHIO-based technique for solving the OPP problem, it is applied to different networks including small 6-bus, IEEE 9-bus, 14-bus, 30-bus, 118-bus, 300-bus, New England 39-bus, and Polish-2383 bus test systems and the results are investigated and discussed.

6.1. Apply the proposed method to a small 6-bus system

To illustrate the OPP objective function and constraints, the proposed technique is applied to the hypothetical 6-bus system illustrated in Fig. 5.

In this test system, bus 3 is assumed as a ZIB, and buses (2, 4, 5, and 6) form radial buses. The cross-links are defined as L3 (between buses 2, and 4), and L8 (between buses 5, and 6). Meanwhile, L7 is not considered a cross-link, as each of the buses (4, and 5) forms its cross-link. In this case, the presence of ZIB, in the system will modify the optimization problem constraints as expressesd by (20).

$$f(x) = \begin{cases} x1 = 1 \\ x_1 \ | x_2 \geq 1 \\ x_2 \ | x_4 \geq 1 \\ x_4 \ | x_5 \geq 1 \\ x_5 \ | x_6 \geq 1 \\ x_2 + x_3 + x_4 + x_5 + x_6 \geq 2 \end{cases} \tag{20}$$

Firstly, the CHIO technique is applied to solve the optimization problem for this test system without considering the ZIB effect, i.e., without taking constraints 3 and 4 into account. The optimum number of PMUs is four units, and the optimum locations for installing them are at buses 1, 2, 3, and 5.

It is necessary to notice that this solution provides the readability of the voltage at any bus, i.e., if a fault occurs at any TL, the voltage value of each bus in the system is available either by direct measurement or by calculation. Assume that a fault occurs in L_3, the voltage at buses (1, 2, 3, and 5) can be measured directly by their own PMUs, while the voltage at bus-4 can be determined via the measured voltage at bus-3 and the current in L_4 that measured by PMU at bus 3. Likewise, the voltage at bus 6 can be determined by utilizing PMU measurements at either bus 3 or bus 5. This means that the system is a full fault observable.

On the other hand, applying the CHIO technique to solve the OPP problem considering the ZIB effect, gives three PMUs as an optimum number and buses 1, 4, and 6 as optimum locations. The three PMUs in this case, are adequate to make the system fully observable. It is important to record that a further solution is obtained by applying the WAO. The other solution states that the PMUs can be installed on buses 1, 4, and 5 and it also achieves full fault observability to the studied system. The results of this case study are summarized in Table 1.

6.2. OPP problem solution for different test systems

The proposed OPP-based-CHIO is represented using MATLAB® programming language and then implemented on several systems including IEEE 9-bus, 14-bus, 30-bus, 118-bus, and 300-bus, in addition to New England 39-bus and Polish 2383-bus test systems. Systems' information and single-line diagrams for all these test systems are available in detail [48,49]. The simulation results for calculating the optimal number of the PMUs and their locations in case of ignoring the ZIB effect are given in Table 2, whereas the results when considering the ZIB effect are shown in Table 3. The optimal solution should be constant for 250 iterations.

It can be noticed from Table 2 that the optimal number of PMUs is in the range of approximately 56 % of the total number of buses for all the test systems. The exception is for the IEEE 9-bus system with the optimal number of PMUs equal to 2/3 of the total number of buses as it is a small system with restricted constraints.

6.3. Fault location evaluation

In this section, the fault observability within the OPP solution is evaluated. For this purpose, simulations are performed for the IEEE 14-bus system illustrated in Fig. 6.

6.3.1. Fault observability evaluation

Consider a three-phase fault occurs at $L_{12\text{-}13}$ (the TL connected bus 12 to bus 13) at 40 % of TL length from bus 13. To accurately locate this fault, the current and voltage at the two ends of the TL should be available.

In the case of ignoring the ZIB effect, the optimum locations of PMUs are explained in Fig. 6-a according to results obtained in Table 2. In this case, both V_{13} and $I_{13\text{-}12}$ are measured directly by the PMU installed at bus 13. While V_{12} is determined using the measured voltage at bus 6, and the measured current at $L_{6\text{-}12}$. Also, $I_{12\text{-}13}$ can be calculated by the current $I_{6\text{-}12}$ measured from PMU installed at bus 6. By applying the resulting V_{12}, $I_{12\text{-}13}$, V_{13}, and $I_{13\text{-}12}$ into (7), the index, D, of the fault location is 0.4018 which locates the fault with an accuracy of 99.8274 %.

In the case of considering the ZIB effect, the optimum locations of PMUs are explained in Fig. 6-b according to results obtained in Table 3. In this case, V_{12}, $I_{12\text{-}13}$, V_{13}, and $I_{13\text{-}12}$ can be measured directly from PMUs installed at buses 12, and 13.

Table 4 demonstrates the PMUs responsible for measuring or determining both terminal voltages V_i and V_j and the currents $I_{i\text{-}j}$ and $I_{j\text{-}i}$ for any $TL_{i\text{-}j}$ in the IEEE 14-bus system. The results prove that the system is fully observable by installing the optimum number of PMUs obtained by the proposed CHIO.

Table 1
OPP for the 6-bus test system.

	Optimal PMU number	Optimal PMU location
Ignoring ZIB effect	4	1, 2, 3 & 5
Considering ZIB effect	3	1, 4 & 6
	3	1, 4 & 5

Table 2

OPP results of the proposed CHIO ignoring the ZIB effect.

Test system	Optimal PMU number	Optimal PMU locations
IEEE 9-bus	6	1,2,3,5,6,8
IEEE 14-bus	8	2,4,5,6,8,9,10,13
IEEE 30-bus	16	1,4,5,6,9,10,12,15,17,19,21,24,26,27,28,29
New England 39-bus	20	2,3,4,6,8,10,12,14,16,17,19,20,21,22,24,25,26,29,36,39
IEEE 118-bus	64	1, 5, 6, 8, 10, 11, 12, 15, 17, 19, 21, 23, 26, 27, 29, 32, 36, 37, 38, 40, 42, 43, 44, 46, 47, 49, 50, 51, 52, 54, 56, 59, 61, 62, 64, 66, 68, 70, 72, 73, 75, 77, 79, 80, 83, 85, 87, 89, 90, 92, 94, 96, 100, 102, 103, 105, 107, 109, 111, 112, 114, 116, 117, 118
IEEE 300-bus	168	2, 3, 5, 8, 10, 13, 15, 18, 23, 25, 26, 28, 29, 30, 31, 32, 33, 34, 36, 42, 43, 44, 45, 48, 49, 50, 51, 53, 54, 55, 56, 59, 63, 65, 66, 67, 68, 70, 71, 72, 73, 74, 75, 77, 78, 83, 84, 89, 92, 93, 94, 95, 96, 99, 101, 102, 103, 105, 106, 108, 109, 111, 112, 118, 120, 124, 126, 127, 128, 129, 130, 136, 137, 142, 143, 145, 146, 148, 149, 156, 160, 162, 166, 167, 168, 169, 171, 174, 175, 181, 182, 183, 185, 187, 189, 191, 196, 198, 199, 204, 207, 211, 212, 213, 215, 219, 220, 221, 222, 225, 227, 228, 230, 231, 233, 234, 236, 238, 239, 240, 241, 242, 244, 245, 249, 250, 251, 252, 253, 254, 255, 256, 257, 258, 259, 260, 261, 262, 267, 269, 270, 271, 272, 274, 275, 276, 277, 279, 280, 281, 282, 283, 284, 285, 286, 287, 288, 289, 290, 291, 292, 294, 295, 296, 297, 298, 299, 300
Polish 2383-bus system	1428	Appendix A

Table 3

OPP results of the proposed CHIO by considering the ZIB effect.

Test system	ZIB locations	Optimal number	Optimal PMU locations
IEEE 9-bus	4, 7, 9	6	1, 2, 3, 5, 6, 8
IEEE 14-bus	7	8	2, 4, 5, 8, 9, 11, 12, 13
IEEE 30-bus	6, 9, 22, 25, 27, 28	14	1, 2, 5, 9, 10, 15, 16, 19, 21, 24, 25, 27, 28, 29
New England 39-bus	1, 2, 5, 6, 9, 10, 11, 13, 14, 17, 19, 22	23	1, 3, 4, 5, 6, 7, 9, 10, 11, 13, 14, 16, 18, 19, 20, 21, 22, 23, 25, 27, 28, 29, 30
IEEE 118-bus	5, 9, 30, 37, 38, 63, 64, 68, 71, 81	55	1, 8, 10, 12, 15, 17, 19, 21, 23, 26, 30, 31, 34, 36, 40, 41, 45, 46, 49, 51, 54, 55, 57, 58, 59, 60, 62, 64, 65, 67, 69, 70, 73, 79, 80, 82, 84, 85, 87, 91, 92, 96, 100, 102, 104, 105, 109, 110, 111, 112, 113, 114, 116, 117, 118
IEEE 300-bus	4, 7, 12, 16, 19, 24, 34, 35, 36, 39, 42, 45, 46, 60, 62, 64, 69, 74, 78, 81 82, 85, 86, 87, 88, 100, 115, 116, 117, 128, 129, 130, 131, 132, 133, 134, 144, 150, 151, 158, 160, 164, 165, 166, 168, 169, 174, 193, 194, 195, 210, 212, 219, 226, 237, 240, 244, 263, 267, 268, 269, 270, 273, 278, 290	157	5, 9, 11, 14, 18, 20, 21, 28, 29, 30, 31, 32, 34, 35, 37, 38, 42, 44, 45, 47, 48, 50, 51, 55, 56, 59, 62, 65, 66, 67, 68, 69, 73, 74, 75, 78, 81, 83, 84, 89, 93, 94, 95, 96, 97, 99, 101, 106, 108, 109, 111, 112, 115, 119, 124, 125, 126, 127, 128, 129, 131, 134, 136, 142, 143, 145, 149, 153, 155, 156, 159, 162, 163, 166, 169, 171, 172, 175, 176, 178, 181, 182, 185, 188, 189, 190, 191, 198, 199, 204, 206, 207, 211, 212, 213, 217, 220, 221, 222, 224, 225, 227, 228, 230, 231, 233, 234, 236, 239, 240, 241, 244, 245, 247, 248, 250, 251, 252, 253, 254, 255, 256, 257, 258, 259, 260, 261, 262, 267, 269, 270, 271, 272, 274, 275, 276, 277, 279, 280, 281, 282, 283, 284, 285, 286, 287, 288, 289, 291, 292, 294, 295, 296, 297, 298, 299, 300
Polish 2383-bus system	Appendix A	1368	Appendix A

6.3.2. Statistical evaluation

Many cases are applied to the IEEE 14-bus test system at various fault conditions. These conditions are comprised of different fault types (phase to phase, single-phase to ground, phase to phase to ground and three-phase faults), source impedances, fault resistances (0.1, 10, and 1000 Ohms), fault inception angles (0°, 30°, and 90°), and fault locations (10 %, 50 %, 90 %) of each transmission line. The total number of these cases is 540. The proposed method is evaluated by estimating the percentage error of fault location using Eq. (21).

$$Error\% = \frac{|Estimated\ fault\ location - Real\ fault\ location|}{Total\ length\ of\ transmission\ line} * 100\% \tag{21}$$

Moreover, several performance indices are used in this study to analyze the performance and the assessment of the proposed method is compared with the application of a phasor domain technique based on the fundamental frequency method for fault location described in Ref. [43]. These indices include Mean Absolute Error (MAE) and Root Mean Square Error (RMSE). The maximum and average fault location errors are illustrated in Table 5. Moreover, the average values of the performance indices are illustrated in Fig. 7. It can be observed that; the proposed algorithm has a good result for wide-range fault conditions with slightly average errors of 0.2312 %.

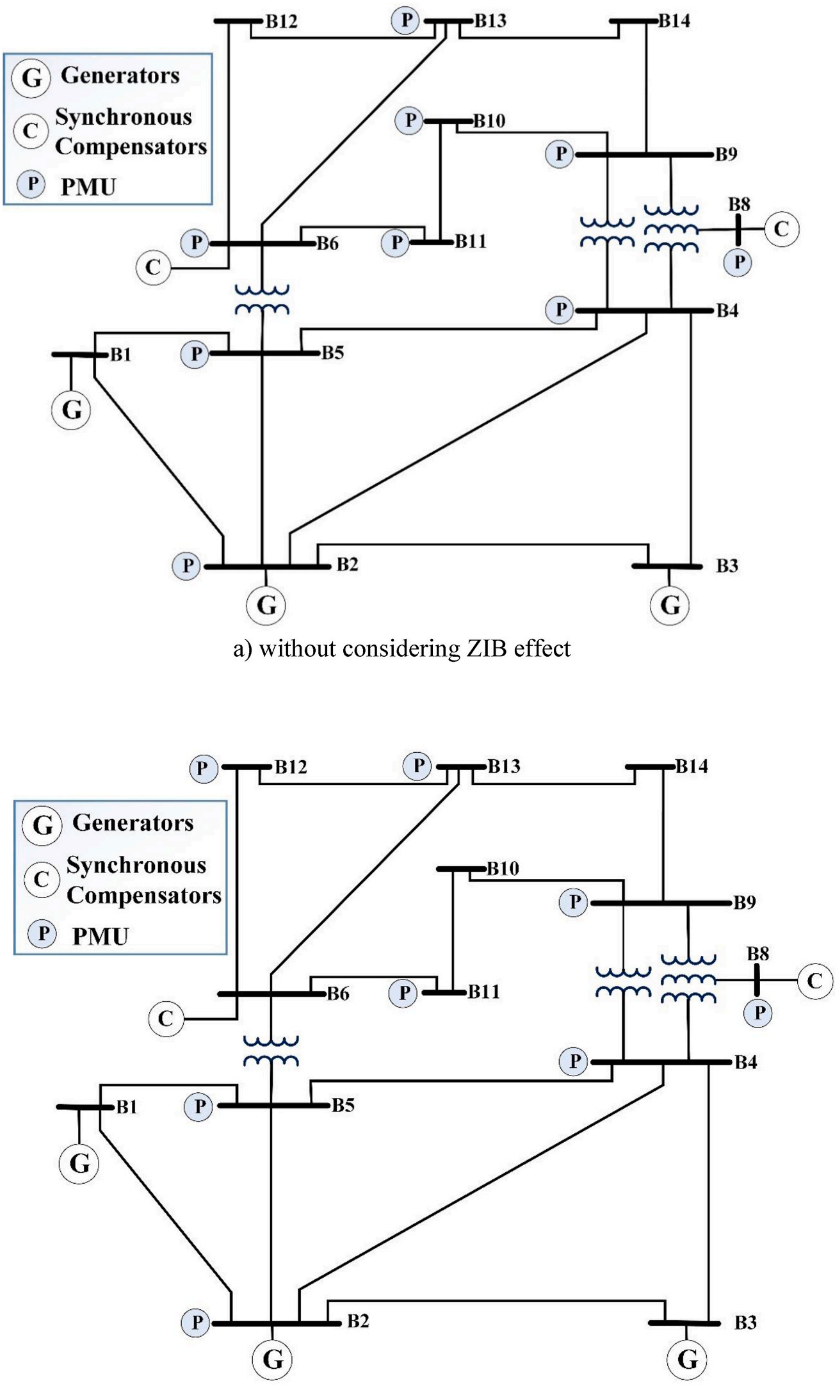

a) without considering ZIB effect

b) considering the ZIB effect

Fig. 6. Distribution of PMUs in the IEEE 14 buses test system.

6.4. OPP result analysis

In this study, a simple, flexible, and fast convergence algorithm is proposed to solve the OPP problem and obtain the optimal PMUs number and their locations in the power systems considering full observability. The impacts of ZIBs and cross-links on the optimal number and locations of the PMUs are studied. Table 6 summarizes the impact of considering the ZIB effect on the optimal PMU number.

Table 4
Fault observability confirmation for IEEE-14 bus system under OPP solution.

Faulty TL	Without ZIB				With ZIB			
	V_j	V_i	$I_{j\text{-}i}$	$I_{i\text{-}j}$	V_j	V_i	$I_{j\text{-}i}$	$I_{i\text{-}j}$
1–2	PMU2	PMU5	PMU2	PMU5	PMU2	PMU5	PMU2	PMU5
1–5	PMU5	PMU2	PMU5	PMU2	PMU5	PMU2	PMU5	PMU2
2–3	PMU4	PMU2	PMU4	PMU2	PMU4	PMU2	PMU4	PMU2
2–4	PMU4	PMU2	PMU4	PMU2	PMU4	PMU2	PMU4	PMU2
2–5	PMU5	PMU2	PMU5	PMU2	PMU5	PMU2	PMU5	PMU2
3–4	PMU4	PMU2	PMU4	PMU2	PMU4	PMU2	PMU4	PMU2
4–7	PMU8/9	PMU4	PMU8/9	PMU4	PMU8/9	PMU4	PMU8/9	PMU4
4–5	PMU5	PMU4	PMU5	PMU4	PMU5	PMU4	PMU5	PMU4
4–9	PMU9	PMU4	PMU9	PMU4	PMU9	PMU4	PMU9	PMU4
5–6	PMU6	PMU5	PMU6	PMU5	P11/12/13	PMU5	PMU11,12,13	PMU5
6–11	PMU10	PMU6	PMU10	PMU6	PMU11	PMU12/13	PMU11	PMU5,12,13
6–12	PMU13	PMU6	PMU13	PMU6	PMU12	PMU11/13	PMU12	PMU5,11,13
6–13	PMU13	PMU6	PMU13	PMU6	PMU13	PMU11/12	PMU13	PMU5,11,12
7–8	PMU8	PMU4/9	PMU8	PMU4/9	PMU8	PMU4/9	PMU8	PMU4/9
7–9	PMU9	PMU4/8	PMU9	PMU4/8	PMU9	PMU4/8	PMU9	PMU4 or 8
9–10	PMU10	PMU9	PMU10	PMU9	PMU11	PMU9	PMU11	PMU9
9–14	PMU13	PMU9	PMU13	PMU9	PMU13	PMU9	PMU13	PMU9
10–11	PMU6	PMU10	PMU6	PMU10	PMU11	PMU9	PMU11	PMU9
12–13	PMU13	PMU6	PMU13	PMU6	PMU13	PMU12	PMU13	PMU12
13–14	PMU9	PMU13	PMU9	PMU13	PMU9	PMU13	PMU9	PMU13

Table 5
Statistical evaluation of studied fault cases in IEEE 14-bus system.

Line	Fault location performance indices %							
	Proposed method				Method in Ref. [43]			
	Max. error	Avg. error	RMSE	MAE	Max. error	Avg. error	RMSE	MAE
1–2	0.3119	0.2356	0.2405	0.1719	0.4060	0.2903	0.2211	0.2903
1–5	0.2531	0.1912	0.1952	0.1395	0.3766	0.2681	0.1852	0.2681
2–3	0.2901	0.2204	0.2248	0.1601	0.3951	0.2827	0.2378	0.2827
2–4	0.3524	0.2683	0.2735	0.1946	0.4262	0.3067	0.2772	0.30665
2–5	0.3011	0.2305	0.2348	0.1665	0.4006	0.2878	0.2569	0.28775
3–4	0.3732	0.2837	0.2893	0.2060	0.4366	0.3144	0.2721	0.31435
4–7	0.3395	0.2527	0.2586	0.1863	0.4198	0.2989	0.26134	0.29885
4–5	0.2725	0.2124	0.2158	0.1515	0.3863	0.2787	0.2245	0.2787
4–9	0.3124	0.2333	0.2386	0.1716	0.4062	0.2892	0.2307	0.28915
5–6	0.3832	0.2879	0.2941	0.2109	0.4416	0.3165	0.2821	0.31645
6–11	0.3312	0.2549	0.2594	0.1835	0.4156	0.3000	0.2432	0.29995
6–12	0.2903	0.2125	0.2181	0.1586	0.3952	0.2788	0.2278	0.27875
6–13	0.3413	0.2235	0.2356	0.1812	0.4207	0.2843	0.2227	0.28425
7–8	0.2981	0.2199	0.2254	0.1632	0.3991	0.2825	0.2359	0.28245
7–9	0.2837	0.1921	0.2006	0.1519	0.3919	0.2686	0.2256	0.26855
9–10	0.3423	0.2417	0.2499	0.1853	0.4212	0.2934	0.2505	0.29335
9–14	0.3152	0.2119	0.2217	0.1685	0.4076	0.2785	0.2389	0.27845
10–11	0.3009	0.2233	0.2286	0.1650	0.4005	0.2842	0.2220	0.28415
12–13	0.2387	0.1957	0.1976	0.1346	0.3694	0.2704	0.18976	0.27035
13–14	0.3112	0.2325	0.2378	0.1710	0.4056	0.2888	0.2671	0.28875

By considering the ZIB effect, the optimal number of PMUs for IEEE 30-bus, 118-bus, 300-bus, and Polish 2383-bus systems is reduced by 12.5 %, 14 %, 6.5 %, and 4.2 % respectively. This is mainly due to the presence of cross-links related to the ZIB in these systems which allows less required number of PMUs. While for the New England 39-bus system, the optimal number of PMUs required for fault observability is increased because it has no cross-links. For both the IEEE 9-bus and 14-bus systems, there is no change in the optimal number of PMUs needed for fault observability when considering or ignoring the ZIB effect due to their small sizing. However, the optimal locations are changed for the IEEE 14-bus system when considering the ZIB effect.

The results acquired by applying CHIO for the OPP problem are compared with the PSO, ILP [40], DE [50], and SQP [51] based methods. In the literature, few methods were applied to large-scale power systems due to their complexity and slow coverage in contrast to the proposed algorithm. Table 7 gives a comparison between the proposed CHIO and other methods. The comparison is executed for the two cases with and without considering the ZIB effect. The results demonstrate that the CHIO effectively reaches the best optimal solution for all the studied systems which can be added to the above-mentioned advantages of applying the CHIO.

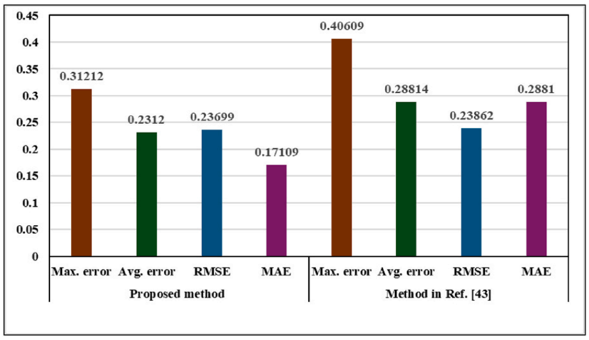

Fig. 7. Accuracy evaluation of the proposed method on studied fault cases in IEEE 14-bus system.

Table 6
Impact of ignoring/considering the ZIB effect on the optimal PMUs number.

	IEEE 9-bus	IEEE 14-bus	IEEE 30-bus	New Eng. 39-bus	IEEE 118-bus	IEEE 300-bus	Polish 2383-bus
Ignoring ZIB effect	6	8	16	20	64	168	1428
Considering ZIB effect	6	8	14	23	55	157	1368

Table 7
Comparison between the proposed CHIO and other methods.

System	Ignoring the ZIB effect					Considering the ZIB effect				
	Method									
	CHIO	PSO	SQP	DE	ILP	CHIO	PSO	SQP	DE	ILP
IEEE 9-bus	6	6	6	N/A	N/A	6	6	6	N/A	N/A
IEEE 14-bus	8	8	8	8	8	8	8	8	8	8
IEEE 30-bus	16	16	17	17	17	14	14	14	14	14
New England 39-bus	20	20	N/A	N/A	N/A	23	23	23	N/A	N/A
IEEE 118-bus	64	64	64	N/A	N/A	55	55	N/A	N/A	N/A
IEEE 300-bus	168	N/A	N/A	N/A	N/A	157	N/A	N/A	N/A	N/A

*N/A: Not available.

7. Conclusion

A novel PMU placement algorithm for observing the faults in power systems has been presented. Simple rules were used to avoid the complications of the numerical analysis. The proposed technique addressed the PMUs' location as an optimization problem. The optimization algorithm based-CHIO was applied to attain the optimum locations and minimum number of PMUs in the power system. The effect of ZIBs' information on the solution of the OPP problem has been investigated. The proposed CHIO was successfully applied to different IEEE test systems including IEEE-9 bus, 14-bus, 30-bus, 118-bus, and 300-bus, New England 39-bus, and Polish 2383-bus systems. Simulation results showed that any fault in any TL can be located using a limited number of PMUs which is fewer than the total bus number of the power system. Less number of PMUs needed for full fault observability was achieved compared to both PSO and ILP-based techniques as confirmed by the results. The results proved that the system was fully observable by installing the optimum number of PMUs as determined by the proposed CHIO and the fault has been located with a precious accuracy of more than 99 %. Therefore, the proposed method is applicable to electrical power systems that are required to be fully observable. The uncertainty of network parameters and PMU communication channels are additional factors that should be considered in future work.

Data availability

Data included in article/referenced in article.

Ethical approval and consent to participate

Review and/or approval by an ethics committee was not needed for this study because it is an Electrical technical paper.

CRediT authorship contribution statement

Mohammed A. Alghassab: Writing – original draft, Validation, Investigation, Funding acquisition, Data curation. **Ahmed Y. Hatata:** Writing – review & editing, Visualization, Methodology, Conceptualization. **Ahmed H. Sokrana:** Writing – original draft, Validation, Software, Data curation, Conceptualization. **Magdi M. El-Saadawi:** Writing – review & editing, Validation, Supervision, Methodology, Conceptualization.

Declaration of competing interest

The authors declare that they have no known competing financial interests or personal relationships that could have appeared to influence the work reported in this paper.

Acknowledgment

The authors extend their appreciation to the deanship of scientific research at Shaqra University for funding this research work.

Appendix

Appendix
OPP results of applying the proposed CHIO on the Polish 2383-bus system ignoring/considering the ZIB effect

Number of Terminal buses	500
Location of Terminal buses	57,58,72,97,109,110,119,122,136,137,146,153,180,181,185,196,197,204,205,231,232,251,252,268,270,271,276,292,301,302,313,327,328,329,330,331,358,362,382,383,390,391,397,398,399,400,402,403,414,418,419,421,422,435,436,449,450,453,454,466,469,470,479,480,495,496,498,499,513,521,522,541,561,562,574,580,597,599,608,673,681,761,767,786,787,788,789,790,791,793,800,801,803,805,806,810,811,816,818,823,824,828,831,832,841,842,843,844,845,846,847,848,853,854,863,867,868,873,875,880,881,884,897,902,907,922,925,927,930,931,933,934,935,937,940,941,945,946,950,951,952,955,956,958,960,969,970,976,977,980,983,984,987,988,1000,1001,1002,1005,1006,1009,1010,1013,1014,1015,1016,1022,1023,1027,1028,1029,1032,1033,1034,1035,1036,1037,1038,1041,1042,1046,1047,1048,1056,1060,1061,1062,1064,1067,1068,1072,1073,1080,1085,1090,1091,1100,1109,1110,1116,1118,1124,1125,1126,1128,1130,1134,1135,1137,1150,1152,1157,1159,1160,1164,1165,1172,1173,1174,1176,1177,1180,1186,1187,1197,1198,1208,1210,1211,1218,1221,1224,1225,1238,1242,1246,1247,1252,1254,1255,1258,1263,1264,1270,1272,1273,1280,1281,1286,1287,1296,1297,1299,1300,1302,1304,1305,1314,1316,1317,1321,1322,1324,1327,1332,1333,1340,1341,1349,1350,1352,1361,1364,1370,1377,1386,1387,1391,1395,1396,1400,1404,1405,1406,1409,1412,1428,1429,1433,1434,1437,1438,1441,1442,1446,1447,1455,1456,1457,1458,1464,1465,1466,1471,1472,1473,1474,1480,1481,1493,1496,1497,1509,1510,1516,1519,1521,1529,1530,1541,1542,1547,1550,1551,1554,1555,1558,1559,1567,1568,1588,1590,1591,1596,1597,1604,1611,1614,1615,1621,1626,1627,1630,1631,1636,1648,1665,1670,1671,1672,1677,1678,1685,1692,1695,1696,1698,1699,1706,1707,1708,1710,1711,1713,1714,1718,1721,1722,1725,1732,1738,1740,1741,1749,1750,1751,1754,1765,1768,1769,1770,1771,1774,1779,1780,1785,1792,1798,1799,1800,1803,1805,1806,1808,1811,1813,1815,1816,1817,1821,1841,1842,1849,1851,1852,1857,1858,1866,1870,1872,1879,1887,1890,1896,1899,1905,1908,1909,1915,1928,1936,1937,1938,1940,1941,1954,1958,1961,1972,1973,1979,1980,1982,1994,1997,2003,2004,2005,2008,2009,2016,2017,2019,2024,2026,2028,2030,2031,2039,2040,2051,2053,2057,2062,2063,2081,2082,2083,2094,2109,2110,2111,2115,2128,2130,2144,2148,2149,2153,2162,2163,2176,2181,2182,2183,2189,2201,2207,2219,2252,2253,2266,2277,2289,2291,2297,2301,2302,2307,2312,2314,2315,2320,2325,2337,2346,2364,2369,2370,2371,2373
Number of ZIB	557
Location of ZIB	1,2,3,4,5,6,7,8,9,11,12,13,14,15,19,20,21,22,23,24,25,26,27,28,32,33,34,35,36,37,38,39,40,46,47,48,49,50,51,52,53,54,55,56,59,60,61,62,66,68,69,70,71,72,73,74,75,76,77,78,79,80,81,82,88,89,90,91,92,94,96,98,99,100,101,102,106,107,108,112,113,114,115,116,117,118,119,120,121,122,128,129,130,133,134,135,136,137,138,141,142,143,144,145,146,147,148,149,150,151,152,153,154,155,156,157,158,159,160,161,162,163,164,165,166,167,168,169,170,171,172,173,174,175,178,179,181,182,194,204,243,280,309,310,312,321,322,332,336,355,361,362,374,375,449,450,470,513,516,517,518,519,539,546,564,565,568,569,576,587,614,617,634,644,645,662,663,682,726,727,734,751,777,786,789,791,797,799,800,801,806,807,812,817,819,821,822,825,826,829,833,836,840,844,848,854,855,856,863,864,869,874,876,879,880,881,885,893,898,903,915,916,

(continued on next page)

Appendix (*continued*)

Number of Terminal buses	500
	921,923,924,926,927,928,931,932,933,934,936,937,938,940,941,946,953,956,966,967, 969,971,972,977,981,984,985,986,987,989,990,991,1003,1006,1007,1008,1013,1017, 1018,1019,1021,1023,1025,1031,1040,1043,1044,1047,1048,1049,1050,1052,1057, 1062,1063,1065,1069,1070,1081,1085,1092,1093,1095,1096,1098,1101,1108,1111, 1112,1114,1115,1119,1120,1121,1123,1127,1129,1131,1135,1151,1152,1153,1157, 1158,1159,1161,1162,1164,1166,1167,1178,1180,1188,1189,1196,1199,1200,1208, 1209,1212,1213,1219,1222,1225,1226,1227,1230,1231,1239,1243,1248,1252,1253, 1256,1257,1261,1264,1265,1271,1274,1275,1279,1281,1288,1298,1299,1300,1305, 1306,1307,1315,1318,1319,1321,1323,1334,1335,1341,1343,1344,1350,1353,1362, 1365,1370,1371,1376,1378,1382,1383,1384,1392,1394,1396,1397,1400,1401,1407, 1412,1413,1423,1431,1432,1439,1440,1443,1448,1449,1455,1456,1459,1460,1465, 1466,1468,1470,1484,1491,1494,1498,1499,1502,1503,1511,1520,1522,1523,1524, 1531,1532,1539,1548,1560,1561,1562,1563,1564,1569,1570,1577,1581,1583,1589, 1591,1592,1601,1618,1621,1631,1632,1636,1647,1648,1649,1650,1665,1670,1681, 1695,1713,1732,1736,1740,1747,1748,1762,1774,1775,1777,1780,1783,1790,1797, 1802,1811,1812,1814,1822,1823,1835,1840,1846,1851,1865,1872,1877,1878,1880, 1881,1885,1887,1896,1899,1902,1903,1906,1907,1914,1919,1920,1922,1944,1948, 1956,1958,1972,1982,1987,2009,2014,2017,2019,2025,2031,2059,2060,2061,2062, 2063,2064,2065,2066,2067,2068,2069,2070,2071,2072,2073,2074,2075,2076,2077, 2078,2079,2080,2081,2089,2090,2092,2109,2111,2112,2113,2133,2134,2157,2158, 2163,2165,2166,2169,2170,2181,2186,2187,2188,2204,2227,2257,2258,2261,2280, 2314,2325,2340,2357,2362,2365,2366,2367,2377,2378,2380,2381
Ignoring ZIB effect	
Optimal number of PMU	1428
Optimal locations of PMU	1,4,5,6,9,10,11,12,13,17,21,23,26,29,30,34,36,42,48,49,51,53,56,57,58,60,61,65,68,69,70, 72,74,76,77,79,80,81,86,88,92,97,99,101,104,105,106,108,109,110,113,116,117,119,122, 128,129,131,133,135,136,137,138,139,142,144,146,147,151,153,154,157,158,159,160,161, 162,165,166,168,169,171,172,178,180,181,182,183,185,186,187,192,193,194,196,197,198, 199,201,202,204,205,207,215,217,219,222,223,224,225,226,227,228,229,231,232,233,237, 249,250,251,252,254,255,256,257,259,260,264,268,269,270,271,275,276,277,280,282,284, 285,287,290,291,292,296,297,299,301,302,304,305,307,308,309,310,312,313,314,318,321, 322,323,324,326,327,328,329,330,331,333,334,335,336,337,344,345,346,349,352,353,355, 357,358,361,362,363,364,366,369,370,371,372,373,374,378,379,380,382,383,384,388,390, 391,394,397,398,399,400,402,403,408,409,412,414,415,418,419,420,421,422,423,425,430, 431,432,433,434,435,436,438,441,442,444,446,449,450,452,453,454,455,456,459,460,462, 464,466,467,468,469,470,472,473,474,475,476,477,479,480,481,484,485,487,490,491,492, 493,494,495,496,498,499,500,502,505,508,511,512,513,516,517,521,522,526,527,531,534, 536,539,541,542,545,547,556,557,558,561,562,565,572,574,576,577,580,581,582,583,587, 588,591,592,593,594,596,597,599,600,601,603,605,607,608,611,612,613,614,617,618,620, 621,625,626,627,629,631,632,634,635,640,643,647,649,650,651,653,654,655,658,659,666, 667,669,670,672,673,674,676,677,678,679,681,682,683,685,686,689,690,691,692,695,696, 697,698,699,700,704,705,708,710,711,712,714,715,717,718,720,722,723,724,727,728,730, 731,733,734,735,737,738,739,740,741,742,745,746,747,750,751,752,755,758,759,761,762, 763,765,766,767,769,770,771,773,776,778,780,781,782,785,786,787,788,789,790,791,792, 793,797,798,799,800,801,803,805,806,807,808,810,811,812,813,815,816,817,818,819,820, 821,823,824,825,826,827,828,830,831,832,833,835,836,838,839,841,842,843,844,845,846, 847,848,849,851,852,853,854,857,859,860,862,863,864,866,867,868,870,871,873,875,880, 881,883,884,885,887,888,890,891,897,898,902,905,906,907,909,911,913,916,921,922,923, 925,927,929,930,931,932,933,934,935,937,940,941,942,945,946,947,948,949,950,951,952, 954,955,956,957,958,960,963,965,966,967,968,969,970,973,974,975,976,977,979,980,983, 984,985,987,988,989,991,992,993,995,996,1000,1001,1002,1004,1005,1006,1008,1009, 1010,1011,1012,1013,1014,1015,1016,1018,1019,1020,1021,1022,1023,1027,1028,1029, 1031,1032,1033,1034,1035,1036,1037,1038,1039,1041,1042,1043,1044,1046,1047,1048, 1051,1052,1053,1055,1056,1057,1059,1060,1061,1062,1064,1066,1067,1068,1072,1073, 1074,1075,1076,1077,1080,1081,1083,1084,1085,1086,1088,1090,1091,1092,1095,1096, 1097,1098,1100,1102,1103,1104,1106,1107,1108,1109,1110,1111,1114,1115,1116,1118, 1119,1121,1124,1125,1126,1127,1128,1130,1134,1135,1136,1137,1138,1139,1140,1141, 1144,1147,1148,1149,1150,1152,1153,1154,1156,1157,1158,1159,1160,1162,1164,1165, 1168,1171,1172,1173,1174,1176,1177,1178,1180,1181,1183,1185,1186,1187,1188,1189, 1190,1194,1196,1197,1198,1201,1202,1205,1206,1207,1208,1209,1210,1211,1212,1213, 1214,1218,1219,1220,1221,1224,1225,1226,1229,1230,1231,1232,1233,1234,1235,1237, 1238,1240,1241,1242,1244,1245,1246,1247,1248,1249,1252,1254,1255,1257,1258,1260, 1262,1263,1264,1266,1268,1269,1270,1271,1272,1273,1274,1275,1277,1279,1280,1281, 1285,1286,1287,1289,1290,1292,1294,1296,1297,1298,1299,1300,1301,1302,1304,1305, 1307,1309,1312,1313,1314,1316,1317,1318,1321,1322,1323,1324,1325,1327,1328,1331, 1332,1333,1335,1337,1338,1339,1340,1341,1344,1346,1349,1350,1352,1353,1357,1360,

(*continued on next page*)

Appendix (*continued*)

Number of Terminal buses	500
	1361,1362,1364,1365,1367,1370,1373,1375,1377,1378,1385,1386,1387,1388,1391,1394,1395,1396,1398,1399,1400,1402,1404,1405,1406,1407,1409,1410,1411,1412,1416,1417,1418,1422,1423,1425,1426,1428,1429,1432,1433,1434,1435,1436,1437,1438,1439,1440,1441,1442,1443,1445,1446,1447,1448,1449,1451,1455,1456,1457,1458,1461,1463,1464,1465,1466,1467,1469,1470,1471,1472,1473,1474,1477,1479,1480,1481,1484,1485,1487,1491,1492,1493,1495,1496,1497,1499,1501,1504,1505,1508,1509,1510,1511,1515,1516,1519,1521,1522,1525,1526,1528,1529,1530,1531,1536,1541,1542,1543,1547,1548,1550,1551,1552,1553,1554,1555,1556,1558,1559,1560,1561,1562,1563,1565,1567,1568,1569,1571,1575,1582,1587,1588,1590,1591,1592,1593,1596,1597,1598,1601,1602,1603,1604,1605,1611,1614,1615,1617,1619,1620,1621,1622,1623,1625,1626,1627,1629,1630,1631,1635,1636,1639,1642,1645,1648,1651,1655,1657,1658,1660,1662,1665,1668,1670,1671,1672,1673,1674,1675,1677,1678,1682,1683,1685,1687,1689,1690,1691,1692,1693,1694,1695,1696,1698,1699,1701,1703,1704,1706,1707,1708,1709,1710,1711,1713,1714,1715,1716,1718,1721,1722,1724,1725,1727,1732,1733,1734,1736,1737,1738,1739,1740,1741,1742,1743,1744,1749,1750,1751,1752,1753,1754,1755,1756,1758,1759,1760,1761,1763,1765,1766,1768,1769,1770,1771,1774,1775,1779,1780,1781,1782,1784,1785,1787,1789,1792,1794,1795,1796,1797,1798,1799,1800,1801,1802,1803,1804,1805,1806,1807,1808,1809,1810,1811,1813,1815,1816,1817,1819,1820,1821,1822,1823,1825,1826,1827,1836,1838,1841,1842,1845,1846,1847,1849,1850,1851,1852,1854,1856,1857,1858,1859,1860,1861,1862,1863,1866,1868,1869,1870,1872,1875,1876,1877,1878,1879,1880,1881,1882,1883,1884,1887,1890,1892,1893,1894,1896,1899,1900,1905,1907,1908,1909,1910,1911,1912,1913,1914,1915,1916,1917,1921,1923,1925,1927,1928,1929,1932,1934,1936,1937,1938,1939,1940,1941,1943,1945,1948,1951,1952,1953,1954,1955,1956,1957,1958,1960,1961,1963,1966,1967,1968,1970,1972,1973,1974,1975,1978,1979,1980,1982,1983,1984,1985,1987,1989,1990,1991,1992,1994,1995,1996,1997,1998,1999,2000,2001,2002,2003,2004,2005,2006,2008,2009,2010,2013,2014,2016,2017,2019,2022,2023,2024,2025,2026,2028,2030,2031,2032,2036,2037,2039,2040,2041,2043,2048,2049,2050,2051,2052,2053,2055,2057,2058,2060,2062,2063,2064,2065,2067,2070,2071,2075,2076,2079,2081,2082,2083,2086,2090,2091,2092,2094,2096,2098,2099,2100,2101,2102,2103,2107,2109,2110,2111,2112,2113,2115,2117,2120,2123,2124,2125,2126,2127,2128,2130,2132,2135,2138,2142,2144,2147,2148,2149,2152,2153,2155,2157,2159,2162,2163,2164,2165,2167,2168,2170,2173,2174,2176,2178,2181,2182,2183,2184,2188,2189,2191,2192,2193,2194,2196,2201,2202,2204,2205,2207,2208,2214,2215,2219,2220,2222,2223,2224,2227,2228,2229,2230,2231,2234,2240,2241,2242,2244,2245,2250,2251,2252,2253,2254,2258,2260,2266,2267,2268,2269,2273,2275,2277,2278,2279,2280,2282,2286,2289,2291,2292,2294,2295,2296,2297,2299,2300,2301,2302,2305,2307,2309,2310,2311,2312,2314,2315,2320,2322,2324,2325,2326,2329,2330,2331,2333,2336,2337,2339,2342,2346,2349,2350,2351,2354,2355,2356,2357,2360,2361,2362,2363,2364,2368,2369,2370,2371,2372,2373,2374,2375,2377,2378,2383
Considering ZIB effect	
Optimal number of PMU	1368
Optimal locations of PMU	6,10,12,14,15,16,18,19,23,24,25,29,30,31,32,34,37,38,39,40,41,43,45,46,47,48,54,55,56,57,58,62,63,65,67,68,69,70,72,73,74,75,78,80,81,82,83,89,91,93,94,95,96,97,99,100,101,102,105,106,107,109,110,113,115,116,119,121,122,125,126,127,128,129,132,134,136,137,138,139,140,146,147,149,151,152,153,154,156,157,158,160,163,164,166,168,172,175,176,178,180,181,182,185,189,190,192,193,195,196,197,198,199,200,201,203,204,205,206,210,211,212,213,218,219,220,223,224,225,227,228,229,231,232,233,234,235,237,238,239,240,241,242,244,249,250,251,252,253,258,259,261,262,263,265,266,268,270,271,274,275,276,280,281,285,286,287,289,291,292,293,295,300,301,302,304,305,309,313,314,316,317,320,323,325,326,327,328,329,330,331,337,339,340,341,344,346,349,350,351,352,358,359,360,361,362,363,365,366,370,371,372,374,380,382,383,384,386,388,390,391,393,394,396,397,398,399,400,402,403,405,406,408,409,411,412,413,414,415,417,418,419,420,421,422,427,429,432,433,435,436,439,440,441,443,444,448,449,450,452,453,454,456,457,462,463,465,466,467,468,469,470,472,473,474,477,479,480,481,483,484,488,490,495,496,497,498,499,500,501,502,503,504,505,510,511,512,513,516,521,522,523,524,526,527,528,529,532,533,534,535,537,541,542,543,554,556,557,558,559,561,562,563,564,566,567,570,574,578,579,580,582,588,590,592,594,597,599,601,602,603,605,606,607,608,610,611,612,613,615,617,618,620,624,627,632,638,640,643,644,647,648,652,654,655,656,657,659,660,663,669,670,673,675,676,678,681,682,683,684,685,689,691,693,699,700,704,708,709,710,711,716,719,722,724,727,728,730,733,738,740,741,742,745,746,747,749,751,752,753,757,758,761,762,765,767,768,769,778,779,782,786,787,788,789,790,791,793,797,798,800,801,803,805,806,807,810,811,812,814,816,817,818,819,821,823,824,825,827,828,830,831,832,833,834,837,841,842,843,844,845,846,847,848,849,853,854,856,861,863,864,865,866,867,868,869,871,872,873,875,880,881,883,884,886,887,888,891,892,894,897,899,900,901,902,903,904,906,907,908,913,915,918,919,921,922,923,925,926,927,930,931,933,934,935,937,939,940,941,942,943,945,946,947,948,949,950,951,952,953,954,955,956,958,960,962,964,965,966,967,969,970,973,976,977,980,983,984,985,987,988,992,993,995,998,1000,1001,1002,1003,1005,1006,1007,1008,1009,1010,1013,1014,1015,1016,1017,1019,1020,1022,1023,1027,1028,1029,1031,1032,1033,

(*continued on next page*)

Appendix (*continued*)

Number of Terminal buses	500
	1034,1035,1036,1037,1038,1040,1041,1042,1043,1044,1045,1046,1047,1048,1049,1051,1052, 1053,1055,1056,1057,1060,1061,1062,1063,1064,1066,1067,1068,1072,1073,1076,1079,1080, 1081,1082,1083,1084,1085,1087,1089,1090,1091,1099,1100,1102,1103,1105,1106,1108,1109, 1110,1111,1112,1113,1115,1116,1117,1118,1122,1123,1124,1125,1126,1127,1128,1130,1133, 1134,1135,1137,1138,1139,1140,1141,1142,1143,1147,1148,1149,1150,1151,1152,1154,1155, 1156,1157,1159,1160,1161,1162,1163,1164,1165,1166,1167,1169,1171,1172,1173,1174,1175, 1176,1177,1178,1179,1180,1182,1183,1184,1186,1187,1190,1192,1197,1198,1200,1201,1203, 1204,1205,1208,1209,1210,1211,1212,1214,1215,1217,1218,1221,1222,1224,1225,1231,1232, 1233,1235,1238,1239,1240,1241,1242,1244,1245,1246,1247,1248,1249,1250,1252,1254,1255, 1256,1257,1258,1262,1263,1264,1266,1270,1272,1273,1274,1277,1279,1280,1281,1283,1284, 1285,1286,1287,1289,1292,1293,1294,1296,1297,1299,1300,1302,1304,1305,1306,1314,1316, 1317,1320,1321,1322,1324,1326,1327,1329,1332,1333,1335,1338,1340,1341,1343,1345,1346, 1348,1349,1350,1352,1355,1357,1359,1360,1361,1364,1367,1368,1370,1372,1374,1375,1376, 1377,1382,1384,1385,1386,1387,1391,1392,1393,1395,1396,1398,1400,1403,1404,1405,1406, 1407,1408,1409,1410,1412,1414,1419,1421,1422,1428,1429,1430,1433,1434,1437,1438,1439, 1440,1441,1442,1445,1446,1447,1453,1454,1455,1456,1457,1458,1461,1464,1465,1466,1467, 1468,1469,1471,1472,1473,1474,1475,1476,1479,1480,1481,1482,1485,1488,1489,1491,1492, 1493,1494,1496,1497,1502,1509,1510,1511,1515,1516,1518,1519,1521,1522,1524,1526,1529, 1530,1532,1534,1536,1537,1541,1542,1543,1546,1547,1549,1550,1551,1552,1553,1554,1555, 1557,1558,1559,1560,1565,1567,1568,1572,1574,1576,1577,1580,1582,1584,1586,1588,1590, 1591,1593,1594,1595,1596,1597,1599,1602,1603,1604,1605,1606,1607,1608,1609,1611,1613, 1614,1615,1617,1619,1620,1621,1622,1623,1625,1626,1627,1628,1629,1630,1631,1632,1633, 1635,1636,1637,1643,1644,1648,1650,1652,1655,1656,1664,1665,1666,1667,1669,1670,1671, 1672,1674,1677,1678,1681,1682,1684,1685,1686,1687,1692,1693,1695,1696,1698,1699,1700, 1701,1702,1704,1705,1706,1707,1708,1710,1711,1713,1714,1715,1718,1719,1721,1722,1725, 1727,1729,1731,1732,1734,1735,1736,1738,1739,1740,1741,1742,1743,1744,1745,1749,1750, 1751,1752,1754,1758,1759,1761,1764,1765,1766,1767,1768,1769,1770,1771,1773,1774,1775, 1778,1779,1780,1782,1784,1785,1789,1790,1792,1796,1798,1799,1800,1803,1804,1805,1806, 1808,1809,1811,1813,1815,1816,1817,1819,1821,1822,1823,1824,1826,1827,1834,1836,1837, 1838,1839,1841,1842,1844,1845,1846,1849,1850,1851,1852,1857,1858,1859,1860,1864,1866, 1868,1870,1871,1872,1873,1874,1876,1878,1879,1883,1884,1887,1890,1892,1893,1894,1895, 1896,1897,1898,1899,1904,1905,1906,1908,1909,1912,1915,1918,1919,1920,1922,1924,1925, 1928,1929,1931,1933,1936,1937,1938,1939,1940,1941,1944,1945,1948,1949,1951,1954,1955, 1958,1959,1961,1964,1966,1967,1969,1970,1971,1972,1973,1979,1980,1981,1982,1983,1986, 1994,1997,1998,2001,2003,2004,2005,2006,2008,2009,2010,2012,2014,2016,2017,2018,2019, 2024,2026,2028,2030,2031,2034,2037,2038,2039,2040,2042,2043,2047,2048,2050,2051,2052, 2053,2054,2057,2062,2063,2065,2071,2075,2076,2077,2080,2081,2082,2083,2085,2086,2088, 2089,2091,2093,2094,2100,2101,2107,2109,2110,2111,2115,2116,2120,2122,2123,2125,2126, 2127,2128,2129,2130,2136,2139,2140,2144,2145,2148,2149,2153,2156,2157,2159,2160,2161, 2162,2163,2166,2169,2170,2173,2174,2176,2180,2181,2182,2183,2184,2186,2187,2189,2191, 2192,2194,2195,2196,2197,2198,2199,2201,2205,2206,2207,2208,2209,2210,2211,2212,2213, 2214,2218,2219,2220,2223,2224,2227,2229,2230,2238,2241,2245,2247,2248,2249,2252,2253, 2257,2259,2263,2265,2266,2267,2269,2271,2274,2276,2277,2282,2284,2286,2287,2289,2290, 2291,2292,2293,2294,2295,2297,2299,2301,2302,2306,2307,2309,2310,2311,2312,2314,2315, 2316,2318,2320,2321,2323,2324,2325,2326,2330,2331,2333,2335,2337,2338,2339,2340,2341, 2342,2346,2348,2350,2351,2353,2355,2358,2359,2364,2365,2366,2368,2369,2370,2371,2372, 2373,2374,2375,2377,2380,2381

References

[1] G. Muthiah, M.D. Manivannan, H. Ramadoss, S. Chenniappan, Distribution phasor measurement units (PMUs) in smart power systems, Artificial Intell.-Based Smart Power Syst. (2023 Jan 25) 311–325, https://doi.org/10.1002/9781119893998.ch16.

[2] G. Paramo, A. Bretas, S. Meyn, Research trends and applications of PMUs, Energies 15 (15) (2022 Jul 22) 5329, https://doi.org/10.3390/en15155329.

[3] A. Pazderin, I. Zicmane, M. Senyuk, P. Gubin, I. Polyakov, N. Mukhlynin, M. Safaraliev, F. Kamalov, Directions of application of phasor measurement units for control and monitoring of modern power systems: a state-of-the-art review, Energies 16 (17) (2023 Aug 26) 6203, https://doi.org/10.3390/en16176203.

[4] A.R. Kulkarni, M.S. Ballal, Synergism of synchrophasor measurements and data analytics for enhancing situational awareness of power grid, Comput. Electr. Eng. 93 (2021 Jul 1) 107231, https://doi.org/10.1016/j.compeleceng.2021.107231.

[5] S. Shankar, K.B. Yadav, A. Priyadarshi, V. Rathore, Study of phasor measurement unit and its applications, in: Recent Advances in Power Systems, Springer, Singapore, 2021, pp. 247–257, https://doi.org/10.1007/978-981-15-7994-3_22, 699(1.

[6] S.K. Bairwa, S.P. Singh, Phasor measurement unit application-based fault allocation and fault classification, Int. J. Adv. Appl. Sci. 12 (1) (2023 Mar) 15–26, https://doi.org/10.11591/ijaas.v12.i1.pp15-26.

[7] M. Netto, V. Krishnan, Y. Zhang, L. Mili, Measurement placement in electric power transmission and distribution grids: review of concepts, methods, and research needs, IET Gener., Transm. Distrib. 16 (5) (2022 Mar) 805–838, https://doi.org/10.1049/gtd2.12336.

[8] A.K. Sahoo, S.K. Samal, Online fault detection and classification of 3-phase long transmission line using machine learning model, Multiscale and Multidiscip. Model. Exp. Des. 6 (1) (2023 Mar) 135–146, https://doi.org/10.1007/s41939-022-00132-x.

[9] J. Fang, K. Chen, C. Liu, J. He, An explainable and robust method for fault classification and location on transmission lines, IEEE Trans. Ind. Inf. 30 (2023 Jan), https://doi.org/10.1109/TII.2022.3229497.

[10] F. Abbasi, A.A. Abdoos, S.M. Hosseini, M. Sanaye-Pasand, New ground fault location approach for partially coupled transmission lines, Elec. Power Syst. Res. 216 (2023 Mar 1) 109054, https://doi.org/10.1016/j.epsr.2022.109054.
[11] Y. Al Mtawa, A. Haque, T. Halabi, A review and taxonomy on fault analysis in transmission power systems, Computation 10 (9) (2022 Aug 24) 144, https://doi.org/10.3390/computation10090144.
[12] V.N. Ogar, S. Hussain, K.A. Gamage, The use of artificial neural network for low latency of fault detection and localization in transmission lines, Heliyon 9 (2) (2023 Feb 1) e13376, https://doi.org/10.1016/j.heliyon.2023.e13376.
[13] D. Akmaz, M.S. Mamiş, Fault location method on two-terminal transmission line using synchronized time information of traveling waves, Electr. Eng. 104 (2) (2022 Apr) 979–990, https://doi.org/10.1007/s00202-021-01356-9.
[14] D. Sodin, M. Smolnikar, U. Rudež, A. Čampa, Precise PMU-based localization and classification of short-circuit faults in power distribution systems, IEEE Trans. Power Deliv. (2023 Apr 20), https://doi.org/10.1109/TPWRD.2023.3268767.
[15] T. Johnson, T. Moger, A critical review of methods for optimal placement of phasor measurement units, Int. Trans. Electr. Energy Syst. 31 (3) (2021 Mar 1) e12698, https://doi.org/10.1002/2050-7038.12698.
[16] M. Elimam, Y.J. Isbeih, M.S. El Moursi, K. Elbassioni, K.H. Al Hosani, Novel optimal PMU placement approach based on the network parameters for enhanced system observability and wide area damping control capability, IEEE Trans. Power Syst. 36 (6) (2021 Apr 29) 5345–5358, https://doi.org/10.1109/TPWRS.2021.3076576.
[17] A.K. Monton, V. Larioza, M. Pacis, An optimal phasor measurement unit (PMU) placement algorithm with (N-1) contingency using integer linear programming (ILP), in: 2021 IEEE International Conference on Automatic Control & Intelligent Systems (I2CACIS), 2021 Jun 26, pp. 81–86, https://doi.org/10.1109/i2cacis52118.2021.9495901.
[18] B. Cao, Y. Yan, Y. Wang, X. Liu, J.C. Lin, A.K. Sangaiah, Z. Lv, A multiobjective intelligent decision-making method for multistage placement of PMU in power grid enterprises, IEEE Trans. Ind. Inf. 19 (6) (2022) 7636–7644, https://doi.org/10.1109/TII.2022.3215787.
[19] A. Al-Hinai, A. Karami-Horestani, H.H. Alhelou, A multi-objective optimal PMU placement considering fault-location topological observability of lengthy lines: a case study in Oman grid, Energy Rep. 9 (2023 Dec 1) 1113–1123, https://doi.org/10.1016/j.egyr.2022.12.046.
[20] A.A. Laouid, A. Djalab, N. Alaoui, Optimal placement of phasor measurement units considering the topology transformation method, in: Advanced Computational Techniques for Renewable Energy Systems, vol. 14, Springer International Publishing, Cham, 2023 Feb, pp. 469–481, https://doi.org/10.1007/978-3-031-21216-1_49.
[21] N.P. Theodorakatos, A nonlinear well-determined model for power system observability using Interior-Point methods, Measurement 152 (2020 Feb 1) 107305, https://doi.org/10.1016/j.measurement.2019.107305.
[22] A.A. Eladl, A.N. Sheta, M.A. Saeed, M.A. Abido, M.A. Hassan, Optimal allocation of phasor measurement units in distribution power systems, Alex. Eng. J. 61 (10) (2022 Oct 1) 8039–8049, https://doi.org/10.1016/j.aej.2022.01.037.
[23] M.K. Arpanahi, R. Torkzadeh, A. Safavizadeh, A. Ashrafzadeh, F. Eghtedarnia, A novel comprehensive optimal PMU placement considering practical issues in design and implementation of a wide-area measurement system, Elec. Power Syst. Res. 214 (2023 Jan 15) 108940, https://doi.org/10.1016/j.epsr.2022.108940.
[24] R. Babu, V.K. Gupta, K. Subbaramaiah, An approach to unravel the optimal PMU placement problem for full observability of power network in view of contingencies, Int. J. Syst. Assurance Eng. Manag. 13 (3) (2022 Jun) 1170–1186, https://doi.org/10.1007/s13198-021-01412-4.
[25] M.M. Devi, M. Geethanjali, Hybrid of genetic algorithm and minimum spanning tree method for optimal PMU placements, Measurement 154 (2020 Mar 15) 107476, https://doi.org/10.1016/j.measurement.2020.107476.
[26] M. Patel, S. Talati, Optimal PMU placement by improved Cuckoo & PSO method, in: In2021 International Conference on Advances in Electrical, Computing, Communication and Sustainable Technologies (ICAECT, IEEE, 2021 Feb 19, pp. 1–6.
[27] S. Shankar, V. Rathore, K.B. Yadav, A. Priyadarshi, Comparative analysis for optimal positioning of PMU, in: In2021 International Conference on Communication, Control and Information Sciences (ICCISc), 1, 2021 Jun 16, pp. 1–5, https://doi.org/10.1109/iccisc52257.2021.9485008.
[28] P. Mohammadi, S. Mehraeen, H. Nazaripouya, Sensitivity analysis-based optimal PMU placement for fault observability, IET Gener., Transm. Distrib. 15 (4) (2021 Feb) 737–750, https://doi.org/10.1049/gtd2.12055.
[29] K. Mazlumi, H.A. Abyaneh, S.H. Sadeghi, S.S. Geramian, Determination of optimal PMU placement for fault-location observability, in: IEEE Third International Conference on Electric Utility Deregulation and Restructuring and Power Technologies., 2008, https://doi.org/10.1109/drpt.2008.4523724. Apr 6-9:1938-1942.
[30] M.E. Golshan, S.H. Dolatabadi, S.M. Tabatabaei, Determining minimum number and optimal placement of PMUs for fault observability in one-terminal algorithms, IET Gener., Transm. Distrib. 12 (21) (2018 Sep 17) 5789–5797, https://doi.org/10.1049/iet-gtd.2018.5906.
[31] N.J. Marand, R.M. Chabanloo, M. Fallah, Optimal placement of voltage measurements for wide-area fault location observability considering the uncertainty of network parameters, Elec. Power Syst. Res. 164 (2018 Nov 1) 79–88, https://doi.org/10.1016/j.epsr.2018.07.036.
[32] M.M. Devi, M. Geethanjali, A.R. Devi, Fault localization for transmission lines with optimal Phasor Measurement Units, Comput. Electr. Eng. 70 (2018 Aug 1) 163–178, https://doi.org/10.1016/j.compeleceng.2018.01.043.
[33] M. Eissa, A. Kassem, Hierarchical Clustering-based optimal PMU placement for power system fault observability, Heliyon 4 (8) (2018 Aug 1) e00725, https://doi.org/10.1016/j.heliyon.2018.e00725.
[34] S. Almasabi, J. Mitra, A fault-tolerance-based approach to optimal PMU placement, IEEE Trans. Smart Grid 10 (6) (2019 Jan 30) 6070–6079, https://doi.org/10.1109/tsg.2019.2896211.
[35] F. Martínez-Álvarez, G. Asencio-Cortés, J.F. Torres, D. Gutiérrez-Avilés, L. Melgar-García, R. Pérez-Chacón, C. Rubio-Escudero, J.C. Riquelme, A. Troncoso, Coronavirus optimization algorithm: a bioinspired metaheuristic based on the COVID-19 propagation model, Big Data 8 (4) (2020 Aug 1) 308–322, https://doi.org/10.1089/big.2020.0051.
[36] S. Safiullah, A. Rahman, S.A. Lone, A novel COVID-19-based optimization algorithm (C-19BOA) for multimodal optimization processes, in: Evolution in Computational Intelligence: Proceedings of the 10th International Conference on Frontiers in Intelligent Computing: Theory and Applications (FICTA 2022), Springer Nature Singapore, Singapore, 2023 Apr 26, pp. 211–222, https://doi.org/10.1007/978-981-19-7513-4_19.
[37] A. Salehan, A. Deldari, Coronavirus optimization (CVO): a novel optimization algorithm inspired from the Coronavirus pandemic, J. Supercomput. 78 (4) (2022 Mar) 5712–5743, https://doi.org/10.1007/s11227-021-04100-z.
[38] M.A. Al-Betar, Z.A. Alyasseri, M.A. Awadallah, I. Abu Doush, Coronavirus herd immunity optimizer (CHIO), Neural Comput. Appl. 33 (10) (2021 May) 5011–5042.
[39] M. Alweshah, Coronavirus herd immunity optimizer to solve classification problems, Soft Comput. 27 (6) (2023 Mar) 3509–3529.
[40] S.P. Pokharel, S. Brahma, Optimal PMU placement for fault location in a power system, in: IEEE 41st North American Power Symposium, Starkville, Mississippi, USA, 2009 Oct 4-6, pp. 1–5, https://doi.org/10.1109/naps.2009.5484002.
[41] A.A. Laouid, R.D. Mohammedi, M.M. Rezaoui, A. Kouzou, Optimal PMUs placement to ensure power system observability under various contingencies, Electrotehnica, Electronica, Automatica (EEA) 68 (1) (2020 Jan 1) 76–86.
[42] Y.J. Lee, T.C. Lin, C.W. Liu, Multi-terminal nonhomogeneous transmission line fault location utilizing synchronized data, IEEE Trans. Power Deliv. 34 (3) (2019 Jan 1) 1030–1038, https://doi.org/10.1109/tpwrd.2018.2890337.
[43] Y. Liu, B. Wang, X. Zheng, D. Lu, M. Fu, N. Tai, Fault location algorithm for non-homogeneous transmission lines considering line asymmetry, IEEE Trans. Power Deliv. 35 (5) (2020 Jan 22) 2425–2437, https://doi.org/10.1109/tpwrd.2020.2968191.
[44] A.Y. Hatata, A.H. Helmy, M.M. Saadawi, Advanced wide-area fault location and classification using phasor measurements units, J. Electr. Eng. 17 (3) (2017 Apr 18) 1–10.
[45] K.B. Swain, C.C. Mahato, A brief review on fault detection, classification, and location on transmission lines using PMUs, Int. J. Manag., Technol. Eng. 8 (3) (2018 Dec) 2608–2618.

[46] Mohammad Dalbah LM. Lamees, M.A. Al-Betar, M.A. Awadallah, R.A. Zitar, A modified coronavirus herd immunity optimizer for capacitated vehicle routing problem, J. King Saud Univ. Comput. Inf. Sci. 34 (8) (2022, Sep) 4782–4795, https://doi.org/10.1016/j.jksuci.2021.06.013.
[47] M.S. Pendem, T.K. Nizami, P. Singh, M.S. Honnurvali, Coronavirus herd immunity optimization-based control of DC-DC boost converter, in: InSoft Computing: Theories and Applications, vol. 627, Springer Nature Singapore, Singapore, 2023 Apr 25, pp. 787–797, https://doi.org/10.1007/978-981-19-9858-4_67.
[48] Weckesser T. Research on Power System Dynamics and Modeling. [Online], Available at: https://tweckesser.wordpress.com/power-system-data-and-test-cases/ .
[49] R.D. Zimmerman, C.E. Murillo-Sanchez, R.J. Thomas, "MATPOWER: steady-state operations, planning and analysis tools for power systems research and education," power systems, IEEE Transactions on 26 (1) (Feb. 2011) 12–19, https://doi.org/10.1109/TPWRS.2010.2051168.
[50] T.A. Alexopoulos, N.M. Manousakis, G.N. Korres, Fault location observability using phasor measurement units via semidefinite programming, IEEE Access 4 (2016 Aug 25) 5187–5195, https://doi.org/10.1109/access.2016.2602838.
[51] N.P. Theodorakatos, Fault location observability using phasor measurement units in a power network through deterministic and stochastic algorithms, Elec. Power Compon. Syst. 47 (3) (2019 Feb 7) 212–229, https://doi.org/10.1080/15325008.2019.1580801.